

ORNL
MASTER COPY

MAR 1 1973
DATE

ORNL-4850
Xic

A STUDY OF CORRELATED THERMALLY
ACTIVATED POLARIZATION, CONDUCTION,
AND LUMINESCENCE EFFECTS IN LITHIUM
FLUORIDE AS FUNCTIONS OF IRRADIATION,
DOPING, AND THERMAL HISTORY

(Thesis)

D. E. Fields

P. R. Moran



OAK RIDGE NATIONAL LABORATORY

OPERATED BY UNION CARBIDE CORPORATION • FOR THE U.S. ATOMIC ENERGY COMMISSION

Printed in the United States of America. Available from
National Technical Information Service
U.S. Department of Commerce
5285 Port Royal Road, Springfield, Virginia 22151
Price: Printed Copy \$3.00; Microfiche \$0.95

This report was prepared as an account of work sponsored by the United States Government. Neither the United States nor the United States Atomic Energy Commission, nor any of their employees, nor any of their contractors, subcontractors, or their employees, makes any warranty, express or implied, or assumes any legal liability or responsibility for the accuracy, completeness or usefulness of any information, apparatus, product or process disclosed, or represents that its use would not infringe privately owned rights.

Contract No. W-7405-eng-26

MATHEMATICS DIVISION

A STUDY OF CORRELATED THERMALLY ACTIVATED POLARIZATION,
CONDUCTION, AND LUMINESCENCE EFFECTS IN LITHIUM FLUORIDE
AS FUNCTIONS OF IRRADIATION, DOPING, AND THERMAL HISTORY

(Thesis)

D. E. Fields, Mathematics Division, ORNL
P. R. Moran, Physics Department, University of Wisconsin

This report has been adopted from a dissertation, Influence of Irradiation and Doping on Thermally Activated Polarization and Luminescence in Lithium Fluoride, presented to the Graduate School of the University of Wisconsin in partial fulfillment of the requirements for the degree of Doctor of Philosophy in Physics by David E. Fields

MARCH 1973

OAK RIDGE NATIONAL LABORATORY
Oak Ridge, Tennessee 37830
operated by
UNION CARBIDE CORPORATION
for the
U.S. ATOMIC ENERGY COMMISSION

ACKNOWLEDGEMENTS

The ideas, helpful criticism, and financial aid contributed by Dick Moran during the pursuance of these studies are greatly appreciated - many of the successes of this thesis are to his credit.

Thanks are also due Luis Barroilhet, Row Kasturi, and Dick Moran for their friendly suggestions and support at many times during my stay in Madison. I benefited from discussions with Jerry Wagner and experimental assistance from Jerry Lasky, and learned much in the classrooms of Clarence Docken and John Thompson.

At ORNL, Mack Patterson and Dick McCulloch helped greatly in offering encouragement and consideration in the latter stages of this work.

Bonnie D. McCarter deserves a medal for the perseverance she showed in her struggle to get my handwritten copy into type.

Finally, I offer special thanks to my wife Sharon, who gave patience and understanding in full measure.

The research reported here was supported by a grant from the Graduate School of the University of Wisconsin and in part, during its later stages, by a grant from the National Science Foundation. During the computations leading to the TAC/TL correlation chapter, the author was employed by the Oak Ridge National Laboratory, where he received partial support again from the National Science Foundation in connection with their presidential intern program.

TABLE OF CONTENTS

	<u>Page</u>
Acknowledgement	iii
List of Figures	vii
Abstract	ix
INTRODUCTION	1
CHAPTER I	
Introduction	5
Theory	7
Experimental	13
Discussion	21
Summary	23
CHAPTER II	
Introduction	25
Theory	29
Apparatus	41
Experimental Results	46
Discussions and Conclusions	50
CHAPTER III	57
CHAPTER IV	
Conclusions	67
APPENDIX I	71
APPENDIX II	75
REFERENCES	77

LIST OF FIGURES

<u>Figure Number</u>	<u>Page</u>
1 Relative Thermally Activated Conductivity (Δ) and Thermoluminescence (O) for 160°K Peaks in LiF(TLD-100)	15
2 Relative Thermally Activated Conductivity (Δ) and Thermoluminescence (O) for 270°K Peaks in LiF(TLD-100)	16
3 The Solid Line Shows the Behavior of the Ratio ($e/4\pi q$) for the 160°K Peaks from Eq. (14). The TL results (O) are shown for comparison. The value of ($e/4\pi q$) varies from a maximum of .0346 to a minimum of -.0063 (dimensionless in cgs units)	18
4 The Solid Line Shows the ($e/4\pi q$) Ratio for the 270°K Peak. This ratio varies from a maximum of 2.4, through a minimum of -12.6. The TL(O) behavior is shown for comparison	20
5 End of Cold Finger (F) Showing Samples (S), Copper Mounting Block (B), Electrical Connections for Heater (H), Thermocouple (T), and Sample Electrode (E). The spiral heater (on back surface of block) is not shown	42
6 Block Diagram of Electronics Used for Direct Current Experiments; For Optical Repopulation, the PMT is Replaced by a Mercury Arc Lamp	45
7 Shown on the Same Plot are the .44-eV Feature (Solid Line) Ascribed to Simple Impurity-Vacancy Dipole Relaxation and the .86-eV Feature (Dotted Line) Thought to Result from Relaxation Subsequent to Dipole Aggregation	47
8 The Solid Curve Shows the RITAD Current in a Sample of High-Purity Optical Quality LiF. The dashed curve shows simultaneously recorded thermoluminescence emission	59
9 The Solid Curve Shows the LiF(UV) Direct RITAD Effect and the Dashed Curve Shows Its Subsequent Optical Regeneration	64

A STUDY OF CORRELATED THERMALLY ACTIVATED POLARIZATION,
CONDUCTION, AND LUMINESCENCE EFFECTS IN LITHIUM FLUORIDE
AS FUNCTIONS OF IRRADIATION, DOPING, AND THERMAL HISTORY

David E. Fields

P. R. Moran

ABSTRACT

This work describes three related phases of our investigations of electrical and luminescence phenomena in pure and doped lithium fluoride. First, we consider the simple trapped carrier-free carrier recombination model often used to describe thermoluminescence (TL) and thermally activated conductivity (TAC) experiments. Both TL and TAC curve shapes depend sensitively on parameter values in the model and general separate solutions for them have not been derived. We present arguments that the actual system possesses significant spatial correlation between trapped carriers and optically active recombination centers.

Next, a study is made of thermally activated polarization (TAP) and thermally activated depolarization (TAD) effects resulting from impurity-vacancy dipole reorientation in Mg doped and undoped lithium fluoride in the temperature region $200^{\circ}\text{K} \rightarrow 250^{\circ}\text{K}$. These results are compared to our earlier measurements of a radiation-induced thermally activated depolarization (RITAD) effect in the same samples. We measure reorientation rate activation parameters of activation energy $E_a = .44 \pm .03$ eV and pre-exponential factor $W_0 = 10^{8.5 \pm 1.5} \text{ sec}^{-1}$ for simple divalent impurity-

vacancy dipole reorientation in samples annealed at high temperatures and quenched. Development of a second polarization phenomena having $E_a = .86 \pm .03$ eV and $W_0 = 10^{19 \pm 1.5}$ sec⁻¹ is observed after annealing several days at room temperature and is apparently due to the formation of stable dipole complexes in which dipole-dipole interactions lead to the replacement of E_a and W_0 by temperature-dependent functions. This second feature is observed at a peak temperature only 2.7% higher than the peak temperature of the .44-eV feature, 220°K.

Finally, we report initial observations of a new radiation-induced phenomenon in LiF; a large permanent electrical polarization can be induced in LiF by ionizing radiation. Specific radiation-induced polarizations, after thermal depolarization, can be regenerated optically but not by thermal repolarization. Rate parameters characterizing thermal depolarization differ from those of other thermally activated processes. This effect has a signal-to-noise ratio comparable to simultaneous thermoluminescence measurements, which suggests many practical possibilities.

INTRODUCTION

Ionizing radiation exposure and impurity doping of simple insulating materials produce a variety of thermally activated optical, electrical conductivity, and electrical polarization effects. These phenomena have received recent renewed interest because of their growing utilization in thermoluminescence radiation dosimetry and in electret and charge storage applications, and also because modern sample purity control now offers hope that one might start to understand some of the microscopic physics involved.

The research project described in this thesis pursued three separate, but interrelated, investigations on the widely studied material, LiF. The motivation for these three studies and the basic findings of the research are:

(1) A general model has been proposed to explain thermally activated charge release and transport in irradiated samples.

It involves nonlinear coupled kinetic equations for trapped charges, free carriers, and recombination centers. Numerical integration of these coupled equations for special cases of particular model parameters has shown that approximate solutions normally applied in analyzing experimental data can be substantially in error.

In this study it is shown that, for this general model, an exact analytic correlation expression for TL/TAC structures can be derived. This expression can be studied experimentally to check the validity of the model. Analysis of two well-resolved LiF TL/TAC curves

shows that the model grossly fails in describing the system's behavior. The data trends strongly suggest that the real system might have considerably spatial correlation between trapping and recombination centers.

(2) The second study concerns the kinetic behavior of divalent impurity-vacancy complexes in lightly and heavily doped LiF. The experiments show that the resulting dipoles produce polarization signals that might easily, if not accounted for, interfere with TAC experiments. It is also shown that there are associated radiation-induced electrical effects, but that there are no gross temperature-dependent anomalies in the susceptibility. A study of aggregation effects after initial annealing revealed a slow conversion from apparent dipole reorientation activation energies of about 0.44 eV to a final value of ~ 0.86 eV. This behavior can easily explain the large discrepancies which exist in the literature between NMR relaxation measurements, dielectric loss studies, and thermally activated depolarization experiments. A theoretical analysis shows the observed changes are more probably slight changes in the temperature dependence of the system's activation energy rather than actual large changes in the magnitude of the activation energy. It is shown that this temperature dependence may be due to aggregation of impurity vacancy dipoles.

(3) The final study described looks basically at the inverse of the phenomena described in the first set of experiments. These experiments measure radiation-induced thermally activated depolarization (RITAD) signals generated in LiF. The results show a very strong phenomena with readout signal to noise comparable to that of simultaneous

TL measurements. One dominant RITAD peak can, after initial ionizing irradiation, be optically repopulated. These results suggest important practical application as a radiation dosimetry technique.

The phenomena studied in these investigations were TAP, TAD, TAC, RITAD, TL and optically repopulated RITAD, TAC, and TL. These acronyms refer respectively to Thermally Activated Polarization, Depolarization, and Conductivity, Radiation Induced Thermally Activated Depolarization, and Thermoluminescence.

In the experimental set-up, the sample has electrodes on two opposing surfaces for producing and measuring the electrical transport properties. The sample is mounted along with a thermocouple and heater in a cryostat having windows to permit both irradiation with ionizing radiation or light and to permit optical monitoring using a photomultiplier tube. One may operationally define the effects named above as follows:

TAP The sample is first cooled, and an electric field is applied with a sensitive ammeter in series with the voltage source. The sample is heated as temperature and polarization current are monitored. This technique, applied to study impurity-induced dipolar states in simple materials, has not been previously described in the literature.

TAD The sample is cooled with a field applied, possibly "freezing in" a polarization. The ammeter is connected across the sample and the sample is heated. Resulting depolarization currents have been called ionic thermal currents; thus this procedure has also been known as the ITC technique.

TAC The procedure is identical to that used in TAP, with the addition of an exposure to ionizing radiation at low temperature. There is no applied field while irradiation is in progress. The distinction is usually made that TAP currents arise from dipole reorientation while TAC currents arise from free charge mobility.

RITAD The unpolarized sample is irradiated with ionizing radiation at low temperature and with an external field applied. The sample is heated and depolarization current is observed as in the TAD experiment.

TL The sample is cooled and irradiated with ionizing radiation. As it is heated, thermally activated light emission is monitored using a photomultiplier.

Repopulated effects RITAD, TAC, and TL in LiF were repopulated using ultraviolet light. Optical repopulation of the TAP and TAD effects could not be observed.

Each of the three studies listed above has been written in manuscript form for submission for publication. The third study, Observation of a RITAD Effect in LiF, has in fact already been published. The first three chapters, consequently, are essentially those manuscripts. Chapter One treats our studies on correlated TL and TAC effects, Chapter Two describes investigations on divalent impurity-vacancy dipoles, and Chapter Three documents our discovery of the RITAD effect and the observation of this phenomena in LiF. The effect described in Chapter Three has been designated "external" RITAD to distinguish it from the "internal" RITAD effect recently discovered by Podgorsak and Moran. The final chapter is an overall summary and discussion of the entire series of experiments.

An appendix has been provided to further comment on our measurement of the attempt frequency of $10^{8.5 \pm 1.5}$ given in Chapter II, Table 1. It is shown that if one accounts for the sensitivity of TAP/TAD measurements to dipole rotation times rather than to vacancy jump times (to which NMR quadrupole relaxation, for example, is sensitive) the value measured here is quite reasonable.

CHAPTER I

AN ANALYTICAL AND EXPERIMENTAL CHECK OF A MODEL FOR CORRELATED THERMOLUMINESCENCE AND THERMALLY STIMULATED CONDUCTIVITY

INTRODUCTION

When an insulating material is exposed to ionizing radiation, there is some probability that the charge carriers (electrons and holes) liberated by the radiation will, instead of returning immediately to their ground state, be captured at trapping sites where they are immobile. If the temperature is maintained at a sufficiently low value, the carriers will remain trapped indefinitely, as they can return to the conduction band only when the local energy barrier is overcome.

When the temperature of the sample is allowed to rise, however, these trapped charge carriers are released and may diffuse some distance through the material before returning to their ground state, possibly with the emission of light to yield thermoluminescence (TL). Under the proper experimental conditions, one may also observe a transient thermally activated conductivity (TAC). Other investigators¹⁻⁸ have studied this

effect and have called it thermally stimulated conductivity (TSC). Unfortunately this term, TSC, often causes confusion as it has been used by investigators of electret state depolarization⁹⁻¹¹ to signify "thermally stimulated current." To emphasize that we are here considering a thermally activated current generated by an externally applied voltage source, we prefer the term TAC.

We see that TL and TAC are closely related phenomena. The relationships between correlated TL and TAC have been studied experimentally and theoretically by Bohm and Scharmann¹⁻³ while theoretical work has been done by Kelly and Braunlich (1970),⁶ Braunlich and Kelly (1970),⁷ and Kelly, Laubitz, and Braunlich (1971).⁸ Other studies by Zimmerman¹² have focused on similar correlations between TL and the related TSEE (thermally stimulated exoelectron emission) effect.

In describing these effects, the system is modeled by a set of kinetic equations describing population dynamics of trapped charge carriers and released mobile carriers. Kelly et al., (1971)⁸ have considered one simple model and obtained exact solutions by numerical methods. Their results show that the approximation normally used to solve the equations and analyze experimental data for trapping parameters can easily become highly invalid and give very erroneous results. They conclude that isolated measurements of thermally activated processes are virtually useless for obtaining trap parameters.

This conclusion leaves open the question of whether the model itself offers a reasonably good description of actual TL/TAC systems. Analysis of experimental data by Bohm and Scharmann,¹⁻³ based upon approximate

solutions to model equations, shows that simultaneous TAC and TL measurements do not correlate as predicted. In view of the work by Kelly and Braunlich,⁶⁻⁸ however, this may easily result from invalidity of the assumptions made in obtaining the approximate solutions.

Our interest is in the correlation between TAC and TL in thermally isolated carrier release peaks. We wish to determine if the normally used model is at all satisfactory, quite apart from our ability to generate exact solutions to the model equations. We have found that the model equations yield directly a simple analytic expression for the correlation between TAC and TL curves. No approximate solution is necessary. One can therefore experimentally examine the extent to which the model is appropriate in describing the system's behavior.

We shall first develop the theory for TL/TAC correlations appropriate to this simple model. A description of our experiments on two pairs of well-resolved correlated TL/TAC peaks is next given, followed by a discussion of the application of model predictions to the experimental data.

THEORY

We shall use the notation introduced by Kelly, Laubitz, and Braunlich.⁸ Considering a single isolated TL/TAC "glow peak," we define:

n_c = density of mobile charge carriers

n = density of trapped charge carriers associated with the particular glow peak of interest

f = density of recombination centers associated with the glow peak of interest ($f = n_c + n$)

- M = density of deep traps associated with thermally disconnected peaks of higher activation energies
- N = net trap density associated with peak of interest
- p = temperature-dependent rate associated with carrier release from traps where E is the activation energy and T is temperature and p_0 is temperature independent ($p = p_0 e^{-E/kT}$)
- β = temperature and time independent capture coefficient of an empty trap for a free charge carrier
- γ = temperature and time independent capture coefficient of a recombination center for a free charge carrier
- μ = charge carrier mobility
- η = optical efficiency factor which relates luminescence output to recombination rate.

By "thermally disconnected" we refer to all higher temperature peaks whose detrapping rate is negligibly small at the temperature attained during the readout of the isolated peak under consideration. In our model the decay of trapped carriers is governed by the equation

$$\partial_t n = -pn + \beta n_c (N - n) \quad (1)$$

while the density of recombination centers diminishes according to

$$\partial_t (n + n_c) = \partial_t f = -\gamma n_c (n + n_c + M) \quad (2a)$$

or

$$\partial_t f = -\gamma n_c (f + M). \quad (2b)$$

The next model assumption is that the magnitudes of TAC and TL as functions of time and of temperature may be expressed by

$$\sigma = \text{TAC} = \mu e n_c \quad (3)$$

$$\varphi = \text{TL} = -\eta \partial_t f \quad (4)$$

where μ is the carrier mobility and η is the probability that the decay of a free charge carrier results in the emission of a photon.

Equations (1) and (2) have been solved numerically for special cases by Kelly, Laubitz, and Braunlich.⁸ Their calculations demonstrate that:

- (a) The location of TL and TAC peaks is a function of p_0 , E , M , N , and f .
- (b) The shape of TL and TAC peaks is determined chiefly by β/γ , M , and N .
- (c) The TL magnitude depends on N , f , M (weakly), and η .
- (d) The TAC magnitude is a function of γ , M , N , f , and μ .

M and N are not independent. They conclude that the only quantity one may in general hope to determine uniquely using only TL/TAC data is the activation energy E .

We are interested here in determining what conclusions may be drawn from quantitative TL/TAC correlations where both effects are simulta-

neously monitored. In our approach to the above model we need use only Eqs. (2), (3), and (4). Combining these equations leads directly to the relation

$$\sigma = \frac{e\mu}{\eta\gamma} \frac{\varphi}{M+f} . \quad (5)$$

In the simple model the quantities e , μ , η , and γ are temperature independent, thus, if we take the temperature derivative of Eq. (5) and evaluate at the TAC peak, $T_{\max}(\text{TAC})$, where $\partial_t \sigma = 0$, we have

$$0 = \partial_t \varphi - \frac{\varphi \partial_t f}{M+f} ; (T = T_{\max}(\text{TAC})) . \quad (6)$$

Using the facts that $\partial_t f < 0$ always and $(M+f) > 0$, one sees from Eq. (6) that

$$\partial_t \varphi < 0 ; (T = T_{\max}(\text{TAC})) . \quad (7)$$

This expression indicates that the TL is decreasing at the TAC peak; i.e., that the TAC peak is at a higher temperature than the TL peak. Substituting Eq. (2) into Eq. (6), we have the relation

$$\frac{\partial_t \varphi}{\varphi} = - \gamma n_c ; (T = T_{\max}(\text{TAC})) . \quad (8)$$

These same conclusions may be reached by evaluating equation (5) at the TL peak temperature.

We need not assume above that the quantities γ and μ are individually temperature independent; indeed, it is sufficient for our purposes in

deriving Eqs. (6)-(8) that the ratio μ/γ is not a function of temperature. This is certainly true if we assume a single charged particle recombination picture. We compute the time rate of decrease of f , the recombination center density for the isolated peak due to the current of free carriers, n_c , which diffuse to within a distance R from the recombination center. Designating $E(R)$ the electric field at the effective recombination radius R , and taking $(M + f)$ as the density of recombination centers, we have

$$\partial_t f = - (f + M) \mu E(R) n_c 4\pi R^2. \quad (9)$$

This is physically just the "recombination current which, from Eq. (2), is equal to $(- \gamma n_c (f + M))$. Consequently,

$$\gamma = \mu E(R) 4\pi R^2, \quad (10)$$

and by substituting $E = \frac{q}{R^2}$, where q is the effective recombination center charge, we find

$$\frac{\gamma}{\mu} = 4\pi q. \quad (11)$$

Thus the ratio (γ/μ) depends only upon the recombination center effective charge, q , which must be temperature independent for Eq. (8) to be valid.

We can extract still more useful results from these equations. Integrating Eq. (4) over time from an initial time 0, to a measurement time t , we have

$$\int_0^t (\varphi/\eta) dt' = - \int_0^t (\partial_t f) dt' = f_0 - f, \quad (12)$$

where f_0 is the value of f prior to initiating readout. Solving Eq. (5) for f and substituting the result into equation (12) gives us

$$\int_0^t \frac{\varphi dt'}{\eta} = M_0 - \frac{e\mu}{\eta\gamma} \varphi, \quad (13)$$

where $M_0 = M + f_0$; this is the initial net concentration of recombination centers. We now accept the usual model assumption that η is temperature and time independent, which allows us to factor it from the integral. In contrast to the expressions in Eqs. (6)-(8), however, we may allow $(e\mu/\gamma)$ to be temperature dependent. Using the recombination center effective charge expression in Eq. (11), we find

$$\int_0^t \varphi(T) dt' = \eta M_0 - \frac{e}{4\pi q} \frac{\varphi(T)}{\sigma(T)}. \quad (14)$$

Equation (14) gives the final form of the correlation expression relating the integrated TL at any time to the ratio of TL and TAC signals at that time. We have made no approximations other than those embodied in the detrapping-diffusion-recombination model. Equation (14) allows us to relate experimental data to the parameters ηM_0 and $(4\pi q/e)$. We see that it is independent of detrapping rate $W(T)$, concentration of filled traps (n) and unfilled traps (N_0), and retrapping cross section (β).

Another useful relation, which allows us to evaluate the effective recombination center charge, is obtained by combining Eqs. (2b), (8), and (11):

$$(q/e) = - (\partial_t \dot{\varphi}/\varphi)(1/4\pi\sigma); (T = T_{\max}(\text{TAC})) . \quad (15)$$

EXPERIMENTAL

These preliminary experiments were designed to test the validity of Eq. (14) as a check of the usefulness of the simple model we have described. Our apparatus is similar to that used by Podgorsak et al.,¹³ with the addition of sample contact electrodes to permit measurement of TAC. A more detailed description is provided elsewhere.¹⁵ We used a single crystal sample of commercial lithium fluoride dosimetric material, TLD-100, purchased from the Harshaw Chemical Company. The dominant dopants in this material are divalent ions, particularly magnesium and alkaline earths, together with some aluminum and titanium activators.

The LiF system was chosen for these studies due to its having been well studied; Bohm and Scharmann (1971) were able to derive a theoretical fit to TL/TAC shapes for a pair of correlated peaks observed at 140°K based upon approximate phenomenological solutions.

The sample was a chip roughly one cm² in area and .1-cm thick. Immediately prior to irradiation, the sample was heated to 700°K and cooled rapidly to approximately 80°K. The sample was then irradiated with 2-mm Al filtered X-rays from a molybdenum target X-ray tube operated

at 75 kv and 50 mA. Typical irradiation levels in these experiments were in the range of 10^3 rads. A voltage source and a Keithley 610C electrometer were connected in series to the sample electrodes. We could attain more than adequate signal to noise ratios with 30 volts applied to the sample and with the system heated at a roughly constant rate of approximately .5 K/sec. The sample temperature was monitored by a thermocouple hard soldered to the copper sample block. This sample block served as a mounting point for the sample, thermocouple, and heater, and was also the common electrode for TAC experiments. Sample current and light output, which was monitored by a photomultiplier, were plotted simultaneously as functions of temperature using two X-Y plotters. Synchronous timing marks were recorded along with the data on each recorder to allow accurate superposition of TL and TAC data.

Among the recorded data were two sets of quite well resolved correlated TL/TAC peaks. The first, with a peak temperature around 160°K , is shown in Fig. 1. Using the relation¹⁴

$$\frac{E}{kT_m} \approx \ln W_0 \left(\frac{\partial_t T}{T} \right)^{-1} \quad (16)$$

one may show that this peak is the same as that seen by Bohm and Scharmann (1971) at 140°K at a heating rate of $.05^\circ\text{K sec}^{-1}$ and by Podgorsak et al., (1971) at 150°K . The TL/TAC signals were well above noise from 135°K to about 185°K . The second TL/TAC set studied is shown in Fig. 2; this set has a peaking temperature at about 270°K . We discuss first the

ORNL-DWG 72-12825

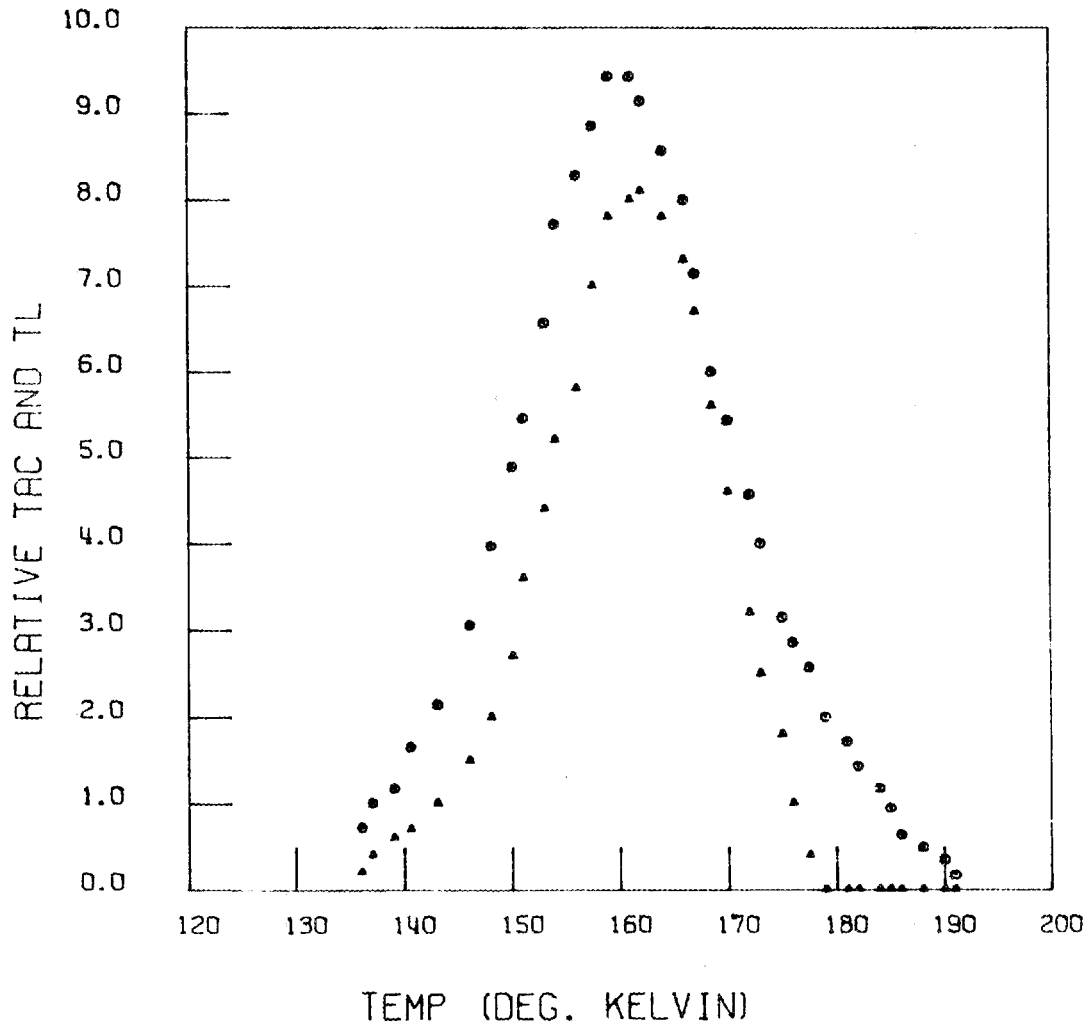


Fig. 1. Relative Thermally Activated Conductivity (Δ) and Thermoluminescence (O) for 160°K Peaks in LiF(TLD-100).

ORNL-DWG 72-12827

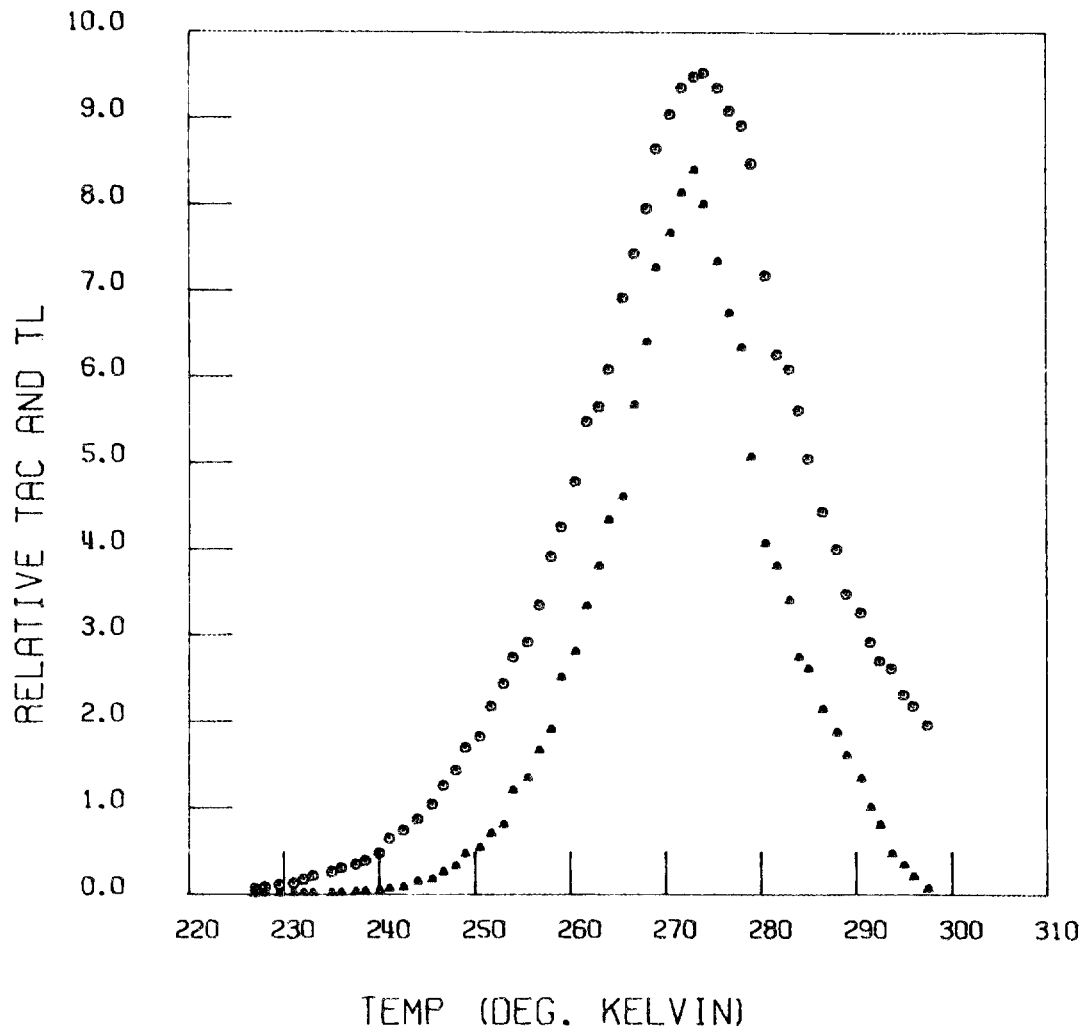


Fig. 2. Relative Thermally Activated Conductivity (Δ) and Thermoluminescence (O) for 270°K Peaks in LiF(TLD-100).

behavior of the 160°K peaks. We note that the temperature shift of TAC to higher temperature than TL, as predicted in equation (7), is very pronounced in Fig. 1. From our measured values at the TAC peak, $\sigma = 2.3 \times 10^{-4} \text{ sec}^{-1}$ (cgs units) and $(\partial_t \varphi / \varphi) = -2.9 \times 10^{-2} \text{ sec}^{-1}$, we use Eq. (15) to calculate the ratio of recombination center effective charge to electronic charge. This yields the value $(q/e) \approx 10$.

To study the full correlation expression of Eq. (14), the data sets were digitized manually as presented in Figs. 1 and 2. A least squares fit of each data set to Eq. (14) was made using a PDP-10 computer and a modified Householder linear least squares procedure.^{16,17} ηM_0 was assumed constant whereas the factor $e/4\pi q$ was fit to a general third-order temperature function $a + bT + cT^2 + dT^3$ where T represents temperature and the other variables were determined. From this procedure we obtained a value of $\eta M_0 = (.89 \pm 1.0) \times 10^{13} \text{ cm}^{-3}$ for the 160°K feature. This value was then substituted back into Eq. (14) and the ratio $e/4\pi q$ was computed and plotted along with the TL signal in Fig. 3. An alternate specification of ηM_0 is obtained from the time interval of TL; by this process a value of $\eta M_0 / \varphi_{\text{max}} = 300 \pm 60 \text{ sec}$ is obtained.

The charge ratio, $(e/4\pi q)$, not only shows a large temperature variation, but even changes algebraic sign. This behavior is roughly indicated by the solid line in Fig. 3 for the 160°K TAC/TL peaks. Obviously, these experimental results grossly disagree with the assumptions of the simple trapped charge-free charge recombination model which led to the correlation expression of Eq. (14). In particular,

ORNL-DWG 72-12828

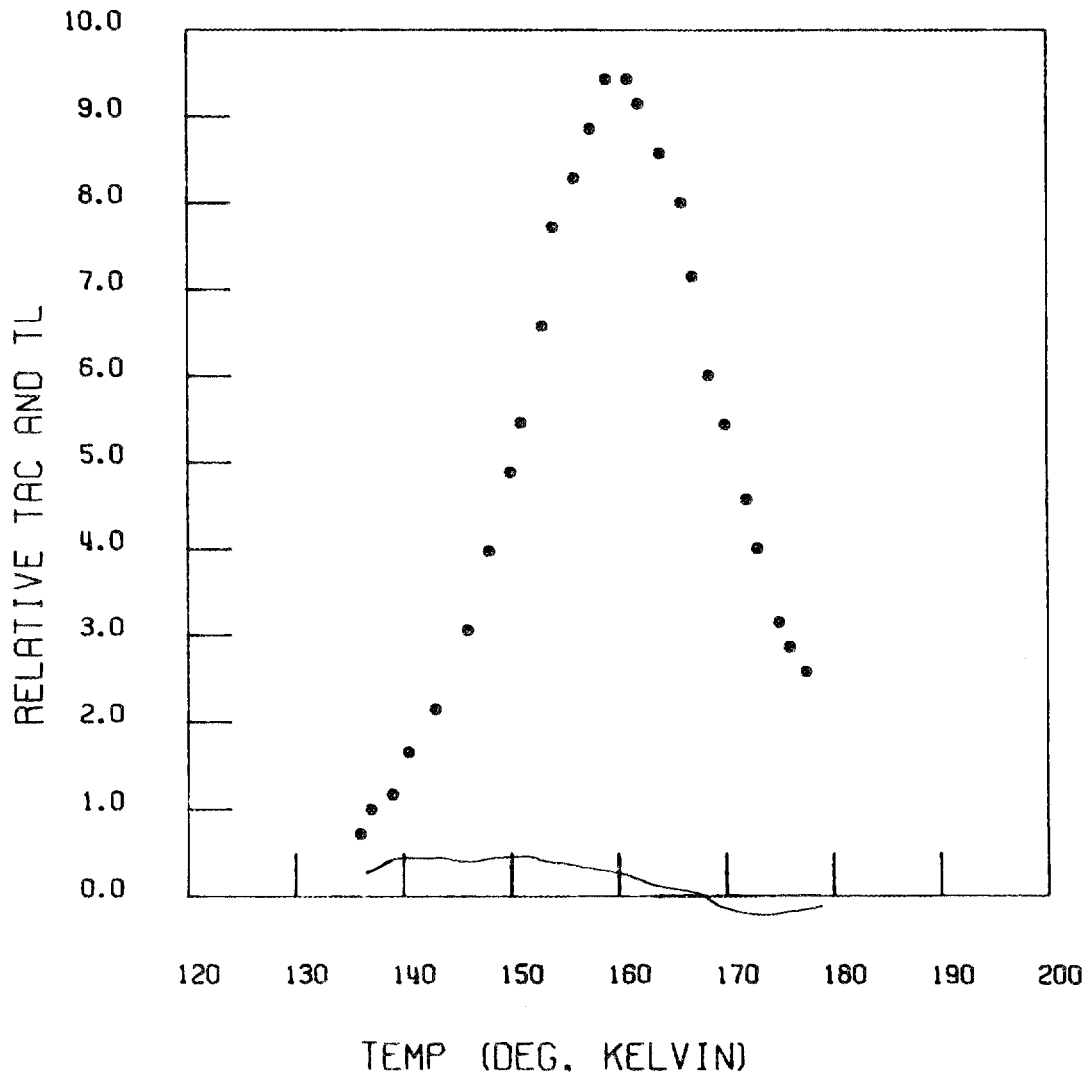


Fig. 3. The Solid Line Shows the Behavior of the Ratio $(e/4\pi q)$ for the 160°K Peaks from Eq. (14). The TL results (O) are shown for comparison. The value of $(e/4\pi q)$ varies from a maximum of .0346 to a minimum of -.0063 (dimensionless in cgs units).

negative values of (q/e) are unphysical. In the initial rise region, from 135°K to 155°K , $(e/4\pi q)$ is reasonably constant at about $(3.3 \pm 0.5) \times 10^{-2}$, or $(q/e) \sim 4$. This value, considering the observed behavior, is in reasonable agreement with the value $(q/e) \sim 10$ obtained previously from Eq. (15).

The observed variation in and the negative going behavior of this ratio are experimentally real. The signal to noise is sufficiently high to insure good statistics, we have made no assumptions such as a single trap "glow peak," and we have verified that the observed effects could not be due to departures from our assumed heating rate. The temperature dependence of q/e is qualitatively the same whether we perform our least squares fit using a constant "average" heating rate or a rate that is a moderately strong function of temperature.

Our second pair of correlated peaks, shown in Fig. 2, was above the noise level from 225°K through around 300°K . When analyzed in a manner identical to that described for the 160°K peaks, the value $\eta M_0 = (3.4 \pm 2.4) \times 10^{13} \text{cm}^{-3}$ was found. The factor $e/4\pi q$ has an initial value $2.4 \pm .5$ and is plotted to show its variations along with TL in Fig. 4. This TL/TAC behavior exhibits an even greater departure from anticipated behavior than does the 160°K peak. Equation (8) is not verified. The TL and TAC maxima lie at apparently the same temperature. The function representing $e/4\pi q$ obtained for this data set had an even larger negative (nonphysical) region than that for the 160°K peak. It does, however, exhibit behavior rather similar to that of the 160°K data set in having

ORNL-DWG 72-12826

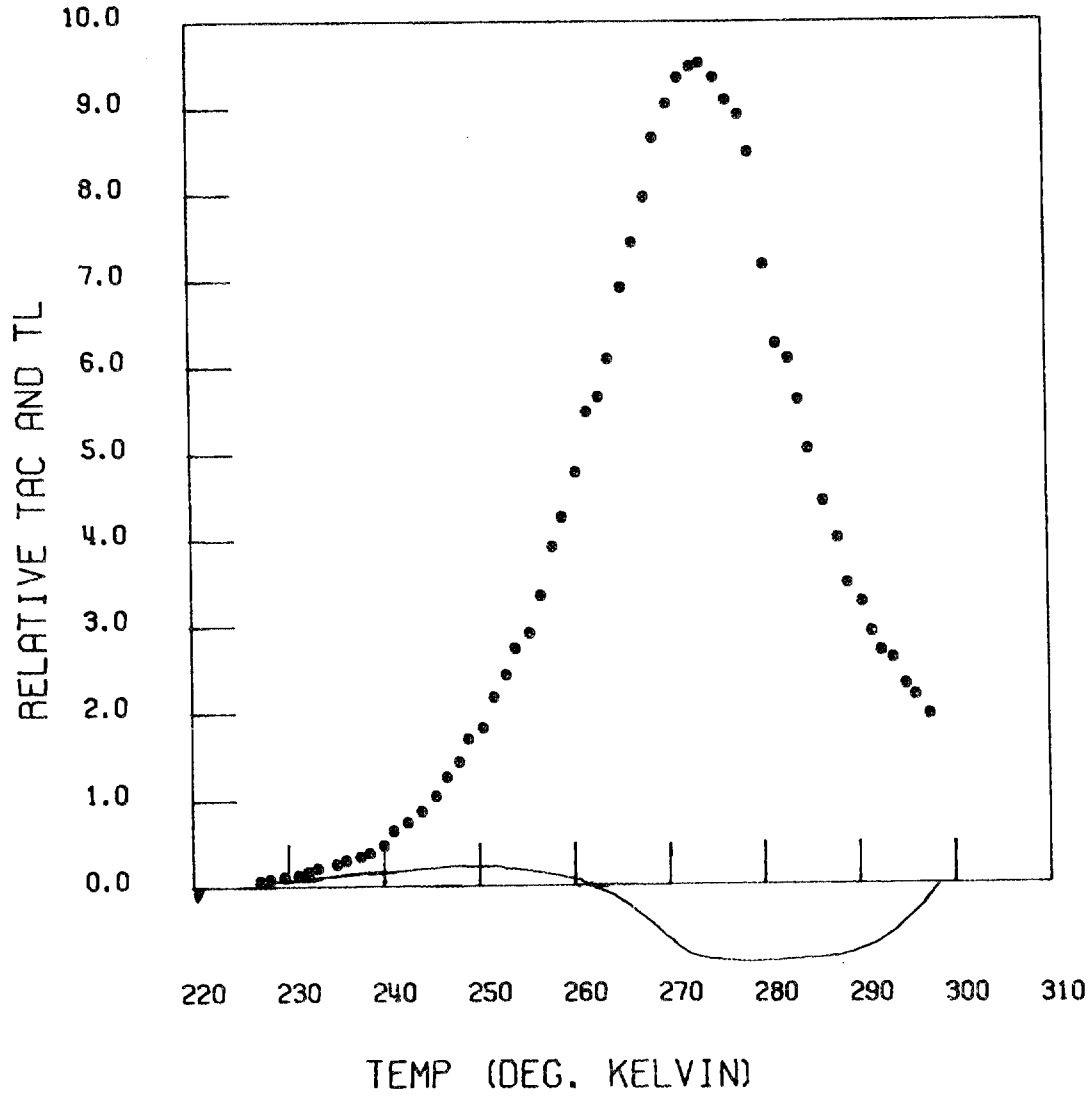


Fig. 4. The Solid Line Shows the $(e/4\pi q)$ Ratio for the 270°K Peak. This ratio varies from a maximum of 2.4, through a minimum of -12.6. The TL(0) behavior is shown for comparison.

an initial "positive" portion followed by a negative going peak. Our leading edge estimation of τ_{M_0} in this case yields a value $\tau_{M_0}/\phi_{\max} = (1. \pm 0.6) 10^3$ sec.

A striking feature of the relative magnitudes of the TL and TAC effects at 160°K and 270°K is that whereas the 270°K TL feature was down from the 160°K feature by more than an order of magnitude (an effect also observed by Podgorsak et al¹³) the 270°K TAC signal was up by two orders of magnitude from its 160°K counterpart.

DISCUSSION

For neither of the two LiF (TLD-100) TL/TAC structures analyzed in these experiments can we obtain correlation behavior between TL and TAC that has reasonable agreement with the expression in Eq. (14) for the simple model. Consequently, further discussion of the detailed numerical values derived would be of little value.

We note that our TL/TAC correlation expression, Eq. (14), rests only on Eq. (2b), which relates the time rate of change of the probability that a given recombination site remains active to the average free carrier concentration, and Eq. (4), which relates the TL to the optical recombination efficiency and the density of recombination centers associated with the peak of interest. In order to reconcile the simple model to our results, one might assume that the optical efficiency, η , is some complicated sharply breaking function of temperature. By such an assumption, one could always force the data to fit Eq. (14). On physical grounds,

however, such a procedure is difficult to justify. We believe a consideration of the qualitative results gives an improved insight into the system's behavior.

First of all, the effective charge of a recombination center, q , in an insulating lattice would be expected to be an electronic charge divided by the material's dielectric constant. For LiF, $\epsilon = 9.0$; we therefore expect $(q/e) \sim 0.1$. This is, for example, a factor of 30 to 90 smaller than the values derived either from the leading slope TL/TAC correlation fit to Eq. (14) or from Eq. (15) for the 160°K TL/TAC results. This suggests to us that the local concentration of carriers near optically active recombination (TL) centers may be much higher than the average bulk carrier concentration, which is measured in the TAC experiment. We speculate, therefore, that, at least in this highly doped TL material, trapped carriers and associated TL recombination centers are spatially correlated to a substantial degree.

We also observed that the ratio of TL to TAC throughout the 270°K feature is less than that ratio for the 160°K feature; that is, a given charge carrier contributes relatively more to TL than TAC for the 160°K peak but more to the TAC than to the TL for the 270°K peak. We might expect this behavior from a system of spatially correlated trapped carriers and recombination centers in which those carriers trapped closest to the recombination centers have a lower activation energy and are therefore observed at a lower temperature than those carriers trapped further from recombination centers.

In the simple model earlier described, the TAC on the high temperature side should fall relatively more slowly than the TL. The reason is that as recombination depletes the TL recombination centers, the detrapped carriers remain free a relatively longer time. Therefore, with respect to the TL output, they contribute relatively more to the TAC on the high temperature than on the low temperature side of the peaks. Experimentally, we find this behavior violated; the high temperature TL does not decrease more rapidly than the TAC. As a result, we derive from Eq. (14) apparent negative values for (q/e) on the high temperature side of the measured peaks. On the other hand, if the TL-active recombination centers are spatially correlated with trapped carriers, then the high temperature TL need not decrease more rapidly than the TAC tails. Such behavior is compatible with the experimental results.

SUMMARY

Our experimental results on correlated TL/TAC peaks in LiF are in striking disagreement with a TL/TAC correlation expression which can be derived exactly from the simple trapped carrier-free carrier-recombination model. We conclude that this model, which is the one normally used to describe TL and TAC measurements, does not provide an adequate description of the system's behavior. These experimental results complement the conclusions of Kelly, Laubitz, and Braunlich⁸ that the approximations often used in analyzing correlated thermally activated data are theoretically unwarranted.

From the observed TL/TAC results, in contrast with the predicted TL TAC correlation expression, we feel that the real system has substantial spatial correlation between trapped carriers and TL-active recombination centers. This could easily account for the discrepancies we observe between experiment and the theoretical expressions which are based upon the assumption of active recombination centers distributed randomly with respect to trapped charges.

CHAPTER II
A STUDY OF THERMALLY ACTIVATED POLARIZATION
EFFECTS IN PURE AND MAGNESIUM
DOPED LITHIUM FLUORIDE

INTRODUCTION

Lithium fluoride is a well-known thermoluminescent (TL) material, and has been studied using this effect by many investigators, both in this country and abroad. More recently, thermally activated conductivity (TAC), also known as thermally stimulated conductivity (TSC), has been detected in the same material and attempts have been made to correlate the TL and TAC effects.^{1,3,7,8} One performs a TAC experiment by exposing a material to ionizing radiation and heating it in the presence of a constant electric field. The movement of charge carriers released from traps in the material is detected as a transient current in the external circuitry which provides the electric field.

It has also been shown that doped lithium fluoride exhibits thermally activated depolarization (TAD).¹⁸⁻²⁰ This effect can be studied by the observation of ionic thermal currents (ITC) which result from the reorientation of impurity-vacancy dipoles. In a TAD experiment, the sample is placed in a large constant electric field and cooled. Upon reaching some low temperature, the electric field is removed. After a short wait for the electronic polarization and possibly the cable polarization to relax, the sample is shunted by a sensitive dc electrometer and heated. The TAD currents observed here are similar in shape to those observed in TAC,

since both processes are thermally activated. Depending on the doping level of the sample used, however, the TAD currents observed may be several orders of magnitude higher than those observed in a TAC experiment.

An experiment obviously closely related to that of TAD is the monitoring of the alignment of impurity-vacancy dipoles in an external applied field as a sample is heated. We call such an experiment thermally activated polarization (TAP). In a TAP experiment, the sample is cooled. Upon reaching some low temperature, a large dc voltage is applied in series with a sensitive electrometer, and the sample is heated. As the polarization builds up, a transient current is observed. This current differs from that seen in the TAD experiment only because, for TAP, the temperature dependent polarizability causes a small background reverse current due to the susceptibility decrease as the sample temperature increases. We see that the conditions for observation of TAC include those necessary for the observation of TAP, and that TAP effects might be expected to lead to the misinterpretation or masking of TAC data. The TAP experiment is useful in itself since it can reveal any anomalies in the temperature dependence of the dipolar susceptibility.

The divalent impurity-vacancy dipoles form a weak electret state in the host material. Electret polarization in some materials is known to be responsive to ionizing radiation through what is called the radio-electret effect.²¹⁻²³ Such effects do exist in our samples and are observed as radiation-induced thermally activated depolarization (RITAD) signals. In RITAD studies, the electric field is applied at low temperatures only during irradiation. The results of our studies of the LiF

RITAD effects have been published elsewhere.²⁴ We will describe again in this paper only those parts which are relevant to the impurity-vacancy dipole orientation effects.

We have carried out TAD/TAP and RITAD studies on pure and doped LiF samples in order to gain information about the following aspects of the impurity-vacancy dipole states:

(1) NMR relaxation studies were performed at this laboratory by Wagner²⁵ on these same LiF Samples. These experiments gave a dipole reorientation activation energy of $0.45 \pm .03$ eV for the 130-ppm Mg-doped sample in the temperature range from 290°K to about 400°K . This disagrees with a value of 0.64 eV obtained from the TAD experiments of Laj and Berge²⁰ in a lower temperature range for much more heavily doped samples, and disagrees with the value of 0.75 eV determined by Grant²⁶ from dielectric loss experiments. Our TAD/TAP studies can hopefully reveal whether the discrepancy is due to different temperature ranges, different measurement techniques, or different sample properties.

(2) The NMR relaxation experiments²⁵ gave data verifying the spectroscopic analysis of dipolar impurity content. Thus our TAD/TAP measurements of the total polarization surface charge, which give the samples susceptibility, can be used to determine the effective dipole length. This reveals something of the structure of the impurity-vacancy complexes.

(3) We have found that the shape of the TAD current vs. temperature undergoes changes depending upon the sample's thermal history. Certain shape changes could conceivably be attributed to dipolar aggregation which produces an anomalously large temperature dependence of the susceptibility.

Since the TAD and TAP signals differ from one another by the temperature derivative of the sample susceptibility, their comparison can reveal whether the effect described above actually exists.

(4) In the following, it is shown that very large TAD/TAP shape changes can be explained by relatively small changes in the temperature dependence of the dipole reorientation activation energy. The TAD/TAP experiments can show whether gross changes in the reorientation rate at a given temperature occur upon dipolar aggregation, or whether it is more likely that the observed effects are due to much smaller temperature dependent changes in the reorientation activation energy.

(5) In subsequent studies, we will examine TL/TAC correlations. It is therefore first necessary to understand the TAP and RITAD behavior of impurity complexes so that these signals can be properly accounted for in the TAC experiments.

The experiments reported here lead us to the following main conclusions: The NMR derived activation energy for complex reorientation agrees with the TAD/TAP activation energy for freshly annealed samples. As the heavily doped sample ages at room temperature, aggregation effects occur, the susceptibility decreases, and a new TAD state evolves which shows a much higher apparent activation energy. The resulting shape change of the TAD curve strongly suggests that the effect is primarily due to a relatively small change in temperature dependence of the activation energy. The dipole polarizability is very large; a simple Curie law calculation yields an rms dipolar length of between one and three lattice constants.

Comparison of TAD and TAP signals, however, shows no observable effect of anomalous susceptibility temperature dependences.

In the following section we outline the theoretical basis for analyzing TAD and TAP signals and treat the behavior expected when activation energies for reorientation are themselves somewhat temperature dependent. The experimental apparatus is next described, followed by a discussion of the experimental results. The final section presents our interpretations and conclusions regarding the TAP/TAD/RITAD effects of the impurity-vacancy dipole states in LiF.

THEORY

General Description of Thermally Activated Polarization Effects

Consider a face centered cubic crystal composed of two monovalent atoms per unit cell and containing positive divalent impurity ions. We assume that these impurity ions substitutionally enter the lattice at positions of positive monovalent ions and that, in order to maintain local charge neutrality, vacancies occupy nearby sites normally occupied by positive monovalent ions. For each such substitutional impurity, there is then an associated dipole moment $\bar{p} = e\bar{d}$ where e is the electronic charge and d is the vacancy to impurity distance. We assume that an electric field E may be present, define $n_{eq}(T)$ as the temperature dependent net dipole moment concentration, and let $n(T)$ be the instantaneous net dipole moment concentration. In this discussion, T refers to temperature while t denotes time.

Taking $W(T)$ to be the temperature dependent dipolar relaxation rate, equilibrium is attained in accordance with the equation

$$\partial_t n = (n_{eq}(T) - n) W(T) . \quad (1)$$

We first find $n(t)$ for those cases where n_{eq} is constant. This case corresponds to isothermal polarization and to the TAD experiment where $n_{eq} = 0$. Equation (1) may be readily integrated between the limits 0 and t with the aid of the integrating factor,

$$\exp \left[\int_0^t W(T) dt' \right] .$$

Using the relation

$$W(t) \exp \left[\int_0^t W dt' \right] = \partial_t \exp \left[\int_0^t W(T) dt \right] \quad (2)$$

we obtain

$$n(t) = n(0) \exp \left[- \int_0^t W(T) dt' \right] + n_{eq}(T) \left\{ 1 - \exp \left[- \int_0^t W(T) dt' \right] \right\} . \quad (3)$$

Thus

$$\begin{aligned} \partial_t n(t) &= W(T) (n_{eq}(T) - n) \\ &= \{n_{eq}(T) - n(0)\} W(T) \exp \left[- \int_0^t W(T) dt' \right] . \quad (4) \end{aligned}$$

The dipole population approaches this equilibrium value in a time determined by the diffusion dynamics of its ionic constituents; we anticipate a reorientation rate of the Arrhenius form,

$$W(T) = 1/\tau(T) = W_0 \exp [-\beta E_a] \quad (5)$$

where W_0 is the rate constant at infinite temperature, E_a is the activation energy for diffusion of one ion about its neighbor associated ion, $\beta = 1/kT$, and $\tau(T)$ is the relaxation time at temperature T .

In a TAD experiment the polarization decays from a level $n(T_0)$, which is determined by a previous polarizing procedure, to $n_{eq}(T) = 0$. In a TAP experiment the aligned dipole concentration is building up to a polarization level $n_{eq}(T)$. We therefore consider a sample in an electric field, E . The polarization in equilibrium with this field, $n_{eq}(T)$, is given by the product of the impurity-vacancy dipole static susceptibility, $\chi(T)$, and the field strength E ,

$$n_{eq}(T) = \chi(T)E \quad (6)$$

For dipoles of molecular dimensions, experimentally attainable field strengths in these studies, and the temperature ranges of interest, $p\beta E \ll 1$. The susceptibility is thus given by the high temperature limit Curie law expression

$$\chi(T) = \Delta N_0 p^2 \beta \quad (7)$$

In Eq. (7), N_0 is the number of impurity dipolar entities per unit volume of the sample, p^2 is the average squared dipole moment per impurity-vacancy complex, and Δ is a geometrical factor related to the microscopic structure of the dipolar complex. For a spherical distribution of dipole directions $\Delta = 1/3$, for vacancies constrained to the nearest neighbor

face centered positions about the divalent ion $\Delta = 2/3$, and for equal populations of nearest neighbor and next-nearest neighbor vacancy positions, $\Delta = 5/9$.

Some Basic Relationships

When the sample's electrodes are held at a constant voltage difference, the current measured in the external circuit in response to changing sample polarization is the displacement current

$$I(T) = A \frac{d}{dt} n, \quad (8)$$

where A is the sample area. We first consider the TAD experiments represented by Eq. (4) with $n_{eq}(T) = 0$. Using Eqs. (4) and (8) we then have

$$I(T) = Q_0 W(T) \exp \left[- \int_0^t W(T) dt' \right], \quad (9)$$

where

$$Q_0 = A \chi(T_p) E_p = A n(T_0) \quad (10)$$

In Eq. (10), E_p is the field strength at which the system was polarized and T_p is the effective polarization temperature, which we shall discuss later.

There are certain basic relationships which are very useful in interpreting the results of a TAD experiment. The first of these is derived from Eq. (8) and shows that the integrated external current is just equal to the stored polarization charge:

$$\int I(T)dt = Q_0 . \quad (11)$$

The TAD current passes through a maximum at temperature T_m , for which an implicit relation may be derived by differentiating Eq. (9) with respect to time and setting $\partial_t I = 0$:

$$0 = \left[\frac{\partial_t W}{W} - W(T_m) \right] . \quad (12)$$

For systems in which $W(T)$ is well described by Eq. (5) over the temperature range of the observed TAD currents, one may evaluate the integral in Eq. (9) as follows:

$$\begin{aligned} \int_0^t W(T)dt' &= \int_0^W (\partial_t W/W)^{-1} dW \\ &= \int_0^W (\partial_t \beta)^{-1} (\partial_\beta \log W) dW . \end{aligned} \quad (13)$$

Now, when the temperature scan is programmed to keep $\partial_t \beta$ constant over the TAD charge release peak, and with $\partial_\beta \log W = -E_a$, one has

$$\begin{aligned} \int_0^t W(T)dt' &= \left[\partial_t W/W \right]^{-1} \int_0^W dW \\ &= \left[\partial_t W/W \right]^{-1} W . \end{aligned} \quad (14)$$

Moreover, the observed charge release peaks are narrow; that is, the temperature breadth of the TAD peaks is very small compared to the peaking temperature, T_m . For narrow peaks, when $\partial_t T$ rather than $\partial_t (1/T)$ is programmed to be constant, one still has an approximately constant $\partial_t \beta$

over the peak. The expression in Eq. (14) remains approximately correct with maximum fractional correction terms equal to the ratio of the temperature breadth to the peaking temperature, T_m . Thus, Eq. (14) remains a useful approximate expression.

One can then use Eqs. (9) and (12) to obtain the peak current:

$$I_{\text{peak}} = I(T_m) = Q_0 (\partial_t \log W) \exp \left[-1 \right]. \quad (15)$$

One can derive the mean temperature breadth δT , of the TAD charge release from the integrated current expression,

$$\begin{aligned} Q_0 &= \int_0^{\infty} I(T) dt = \int I(T) (\partial_t T)^{-1} dT \\ &\approx (\delta T) (\partial_t T)^{-1} I(T_m). \end{aligned} \quad (16)$$

By substituting this relation in Eq. (15), one obtains

$$(\delta T) = (e) (\partial_t \log W)^{-1} (\partial_t T), \quad (17)$$

or an alternative form, using again Eq. (12),

$$(\delta T) = (e) \left[\partial_t T / W(T_m) \right]. \quad (18)$$

From the Arrhenius form in Eq. (5), Eq. (12) can be evaluated for T_m ;

$$(\partial_t T) (E_a / kT_m^2) = W_0 \exp \left[-E_a / kT_m \right], \quad (19)$$

or

$$\left(\frac{E_a}{kT_m}\right) + \log \left[\frac{E_a}{kT_m} \right] = \log \left[W_0 \left(\frac{\partial T}{\partial T_m} \right)^{-1} \right]. \quad (20)$$

Then Eq. (19) may also be expressed as

$$T_m = \left[\left(\frac{\partial T}{\partial T_m} \right) \left(\frac{E_a}{k} \right) \right]^{1/2}, \quad (21)$$

which can be combined with Eq. (18) to see that for narrow peaks, i.e., $(\delta T/T_m) \ll 1$, one has $E_a/kT \gg 1$. Thus Eq. (20) can be written to a good approximation as

$$\left(\frac{E_a}{kT_m}\right) = \log \left[W_0 \left(\frac{\partial T}{\partial T_m} \right)^{-1} \right]. \quad (22)$$

The basic relations derived above will prove useful in interpreting the trend of our experimental data. To determine how $W(T)$ actually behaves over the entire TAD/TAP peak, however, we develop further expressions more suitable for detailed data analysis.

Method of Data Analysis

We discuss first the "leading edge" analysis. If we take the logarithmic derivative of Eq. (9) with respect to β , we find

$$\frac{d \log I}{d\beta} = -E_a + E_a W(T) \left(\frac{\partial T}{\partial T_m} \right)^{-1}. \quad (23)$$

As the second term in Eq. (23) is small for T small compared to T_m , a convenient approximation for the low temperature leading edge may apparently be used to obtain E_a :

$$E_a = - \frac{d \log I}{d\beta} \quad (24)$$

It appears that one might plot $\ln I$ vs. $\frac{1}{kT}$ below T_m and make use of all data until the point of obvious departure from the above linear relationship. Haake²⁷ has shown, however, that if one hopes by this method to obtain values of E_a accurate to 5%, he must stay more than 20 degrees below the peak temperature. This criterion may be shown to be applicable over a wide range of peak temperatures, thus showing this equation to be relatively unhelpful in data analysis. Furthermore, as we see later, there may be more than one TAD component which is unresolved in a single peak. The leading edge analysis does not reveal such complications.

It is for these reasons that we have determined our values of W_0 and E_a starting with Eq. (1). From the recorded current we integrate the output from time t to a later time, t_2 :

$$\int_t^{t_2} (\partial_t n - \partial_t n_{eq}(T)) dt' = \left[n(t_2) - n_{eq}(t_2) \right] - \left[n(t) - n_{eq}(t) \right]. \quad (25)$$

In a TAP run, t_2 is taken as the point where the current crosses zero, i.e., $n(t_2) = n_{eq}(t_2)$, and in a TAD run (where $n_{eq} = 0$), t_2 is simply taken to be so large that the current has dropped well below the noise level.

In either case the first term on the right side of Eq. (25) is zero and, from Eq. (1), we obtain the useful result

$$W(T) = \frac{\partial_t n}{\int_t^{t_2} \left[\partial_t n - \partial_t n_{eq}(t') \right] dt'}. \quad (26)$$

TAD Effect

In the case of a TAD experiment, the external applied electric field is zero. Thus $n_{eq}(T)$ is also zero and Eqs. (5), (9) and (10) give us

$$I(T) = -A\chi(T_p)E_p W_0 \exp \left[-\beta E - \int_{T_0}^T W(T)/\partial_t T dt \right]. \quad (27)$$

Equation (26) may be rewritten, with $\partial_t n_{eq} = 0$ and using Eq. (8), to give

$$1/\tau(T) = W(T) = \frac{I \partial_t T}{\int_T^{T_0} I(T) dT}, \quad (28)$$

which enables us to determine $W(T)$ at various points on the current peak. The slope of $\ln \tau(T)$ vs. $\frac{1}{kT}$ gives us E_a while the intercept gives us W_0 ; alternatively, Eq. (21) may be rewritten as

$$W_0 = \frac{\partial_t T E_a e^{E_a/kT}}{kT_m^2} \quad (29)$$

which gives us the pre-exponential factor W_0 once E_a and T_m are known.

TAP Effect

For a TAP experiment it is $n(0)$ which is zero. Thus we find here that $I(T)$ is given approximately by

$$I(T) = A\chi(T)E W_0 \exp \left[-\beta E_a - \int_{T_0}^T \frac{WdT}{\partial_t T} \right]. \quad (30)$$

In this experiment the $\partial_t n_{eq}$ term does not disappear as it did in the TAD case but in our experiments the $\partial_t \chi$ term correction was experimentally negligible.

Let us first suppose that the dipolar system is well behaved and follows a smooth $(1/T)$ behavior as anticipated in Eq. (7). Then we can make a very useful observation that allows us to still analyze our data by the same method as in the TAD experiment. A data peak has a temperature width at half maximum of roughly 15°K ; our peaking temperatures are around 200°K for these experiments. As we go through one TAP peak the polarization goes from 0 to very close to n_{eq} . Therefore, Eq. (26) gives

$$W(T) \approx \frac{\partial_t n}{\int_t^2 \partial_t n} \left\{ 1 + \frac{15^\circ}{200^\circ} \right\}, \quad (31)$$

and Eq. (28) is seen to be valid for TAP analysis to an accuracy of roughly 10%.

Suppose, on the other hand, that due to some such cause as cooperative interactions among aggregated dipoles, the system susceptibility does not follow the $(1/T)$ behavior of Eq. (7). If $\chi(T)$ has an anomalously large T dependence in the temperature range observed, then Eq. (31) will not hold. In such a case, when Eq. (28) is applied to both a TAD and a TAP run on the same system there may result a large discrepancy signifying the existence of a susceptibility anomaly.

RITAD Effect

As will be explained in the discussion, we believe that the RITAD signals are a radiorelectret polarization of the impurity-vacancy dipoles.

Since this is a special case of TAD, we feel justified in using the same analysis as that applied to TAD.

Temperature Dependent Activation Parameters

There is good theoretical reason to believe that the form given in Eq. (5) for $W(T)$ should be at least approximately correct over a reasonable range of temperatures. In real systems, however, this simple form may not be adequate for describing the observed behavior over a wide temperature range. We note that Eq. (5) can be a general description of $W(T)$ if we allow the activation energy to be temperature dependent.

In particular, we see that Eq. (26) is valid even for an explicitly temperature dependent activation energy, $E_a(T)$. Moran et al.,^{14, 28} have considered the results of such an explicit temperature dependence for the mathematically analogous thermoluminescent experiment. They conclude that, for narrow peaks and first-order kinetics, one has a rate over the observable peak which can be expressed

$$W(T) = W_0^* \exp(-\beta E^*), \quad (32)$$

where

$$E^* = \partial \beta \left[\beta E(\beta) \right], \quad (33)$$

and

$$W_0^* = W_0 \exp \left[-\beta (E^* - E(T)) \right]. \quad (34)$$

That is, the kinetics appear to be governed by an effective activation energy E^* and an effective pre-exponential rate W_0^* . In particular, all the relations discussed previously remain valid if one substitutes E^* for E_a and W_0^* for W_0 .

We especially note the relationship given for E_a/kT_m in Eq. (28). For a slightly temperature dependent E_a , this becomes

$$E^*/kT_m = \log \left[W_0^* \left(\partial_t T/T_m \right)^{-1} \right]. \quad (35)$$

This is particularly interesting since the expressions in Eqs. (33) and (34) for E^* and W_0^* can be substituted into Eq. (35) to give

$$E_a(T_m)/T_m = \log \left[W_0 \left(\partial_t T/T_m \right)^{-1} \right]. \quad (36)$$

A simple physical interpretation is that the temperature dependence of the relaxation kinetics and hence of the TAD/TAP shapes is determined by the logarithmic temperature derivative of the rate function, $E^* = -\partial \beta \log [W(\beta)]$; on the other hand, the peaking temperature, T_m , is predominately determined by the temperature at which the magnitude of $W(\beta)$ becomes comparable to $(\partial_t T/T)$. Thus, within the temperature range of a TAD/TAP peak, two systems might have almost equal values of $W(T)$ and almost equal values of E_a . In one system, however, if E_a is slightly temperature dependent, analysis will yield effective activation parameters E^* and W_0^* quite different from E_a and W_0 . Both systems, nevertheless, will show about the same value for T_m according to Eq. (36).

This conclusion is important here because we believe we can induce temperature dependent activation energies and frequency factors by varying

doping levels and sample treatment so as to cause dipole aggregation. The formation of trimers, aggregates of three impurity vacancy dipoles, has been recognized and studied in several other alkali halides by Cook and Dryden²⁹ and more recently by Capelletti and Okuno.³⁰

We believe the observation of E_a^* and W_0^* rather than E_a and W_0 in samples with a concentration of impurity levels or in samples that have been aged is the reason for the aforementioned apparent discrepancies in the literature.

APPARATUS

Samples studied were primarily pieces of a single ingot of Harshaw LiF doped with 130-ppm magnesium which enters as a divalent impurity ion. Several crystals of TLD-100, a commercially available dosimetry grade LiF crystal also containing magnesium, and of Harshaw H63A high purity optical grade material, LiF(UV), were also examined. Wagner's experiments²⁵ on NMR relaxation in these H63A LiF samples showed divalent impurity-vacancy complexes in a concentration of about 10 ppm.

The samples were cleaved to a cross section of 1-x-1 cm² and approximately 1-mm thickness and cemented by conductive epoxy onto the front surface of a copper block screwed into the base of a stainless steel cole finger. This is shown in Fig. 5. Also to the front surface of this block was affixed one junction of an iron constantan thermocouple referenced to an ice bath. To the back of the copper block was hard soldered a spiral heater consisting of a 1-mm-diam inconel sheath surrounding a .1-mm

ORNL - DWG 72-8091

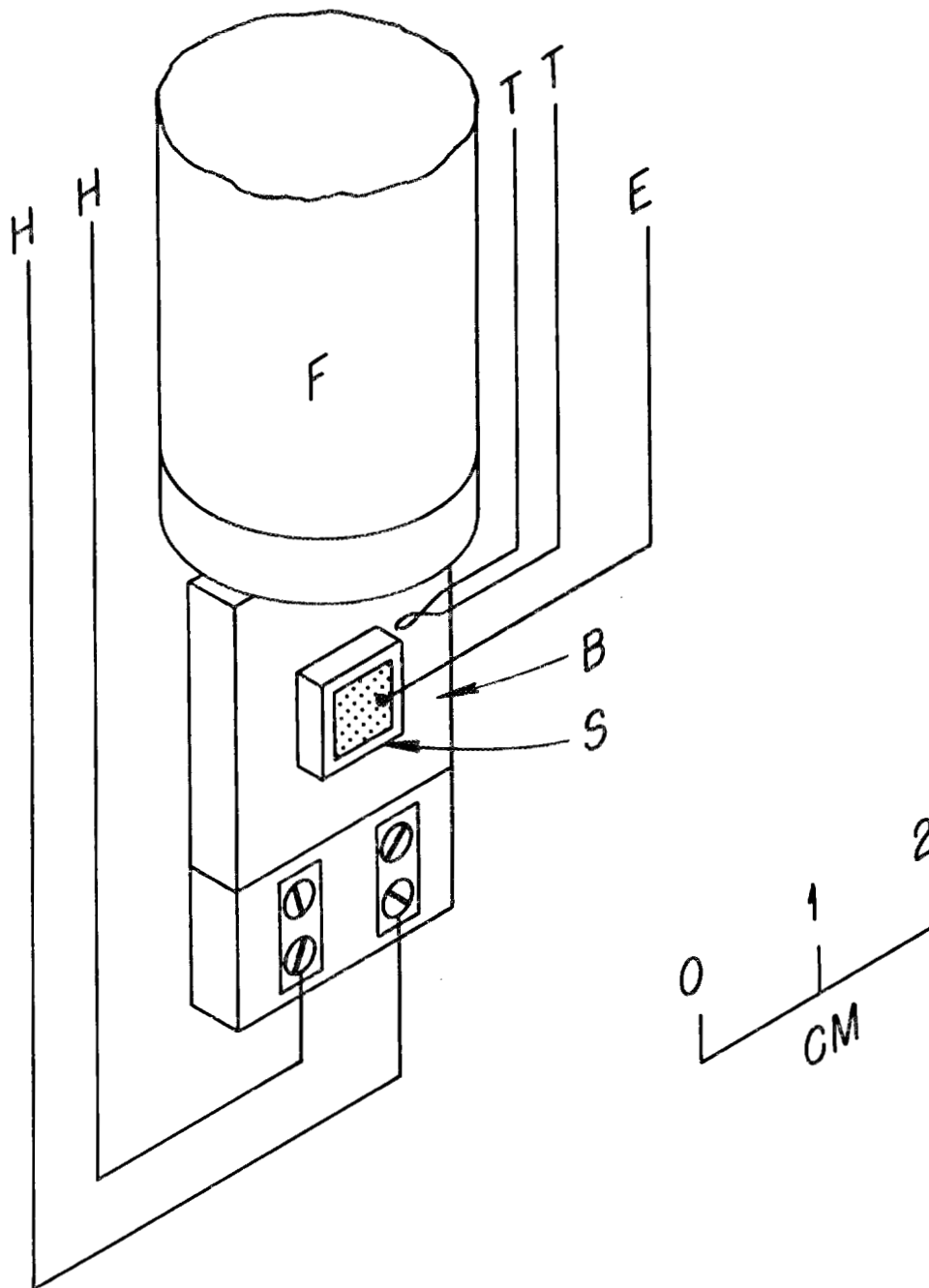


Fig. 5. End of Cold Finger (F) Showing Samples (S), Copper Mounting Block (B), Electrical Connections for Heater (H), Thermocouple (T), and Sample Electrode (E). The spiral heater (on back surface of block) is not shown.

nichrome heater wire from which it was insulated by alumina powder. The heater was constructed using a material available from the Amperex Corporation under the name Thermocoax. We found this a highly satisfactory arrangement; there was intimate thermal contact between the heater and the block, and the heated wire itself was shielded by the outer sheath. This arrangement kept black body radiation of the heated wire from reaching our photomultiplier tube, which was used in a subsequent series of complementary experiments. On the base of the copper block was mounted an insulator formed of machinable ceramic which served as a tie point for heater connections. Excellent thermal contact between the block and sample allowed very high temperature scan rates without problems of temperature lag or gradients in the sample.

Thermocouple wires entered directly through the top flange of our stainless steel vacuum chamber, with epoxy cement used to prevent their being shunted to ground, an arrangement which prevented small offset voltages which tend to develop at cooled vacuum feed through junctions from being a problem. We did use feed through insulators, however, for both heater wires and for the sample sensing electrode wire. The sample's common electrode was grounded through the heater block. All wires except the sample wire were teflon insulated; the sample wire was glass insulated and fixed to the sample surface by silver conductive paint.

An electronic temperature regulator was constructed and used to monitor the thermocouple output and provide a programming voltage for the heater power supply, thus allowing isothermal annealing of the sample to be done to an accuracy of $\pm .1^{\circ}\text{K}$. A block diagram of our circuitry is

shown in Fig. 6. The cold finger and sample assembly was rotatable under vacuum conditions. For all experiments the chamber was evacuated to a pressure of $5 \cdot 10^{-4}$ torr. Cooling was effected by flowing chilled nitrogen gas through the cold finger until the temperature reached 150°K and then by slowly adding liquid nitrogen. This procedure lowered the probability that the bond between the sample and the copper block would be destroyed by thermal stresses.

Our X-ray source was a GE XRD-3 machine operated at 75 kv and 50 ma with a molybdenum target. Filtering consisted primarily of a 2-mm-thick aluminum window on the sample chamber to yield an exposure rate of approximately 100 R min^{-1} at the sample.

A Keithley Model 610C electrometer was used for current monitoring. Output current vs. thermocouple voltage was recorded on an x-y plotter. A timing generator could be coupled into the signal channel to provide time base interval marks. Representative cooling and heating rates were $.2^{\circ}\text{K/sec}$ and $.5^{\circ}\text{K/sec}$ respectively.

As DC measurements were made, the light output of the sample was simultaneously monitored using an EMI 6256 B photomultiplier tube with quartz optics throughout the system. To perform optical repopulation experiments, the photomultiplier could be replaced by a PEK short arc mercury lamp operated at 65 W and backed by a concave mirror. The sample, covered by a transparent electrode, was located 15 cm from the arc and irradiation times were 30 minutes.

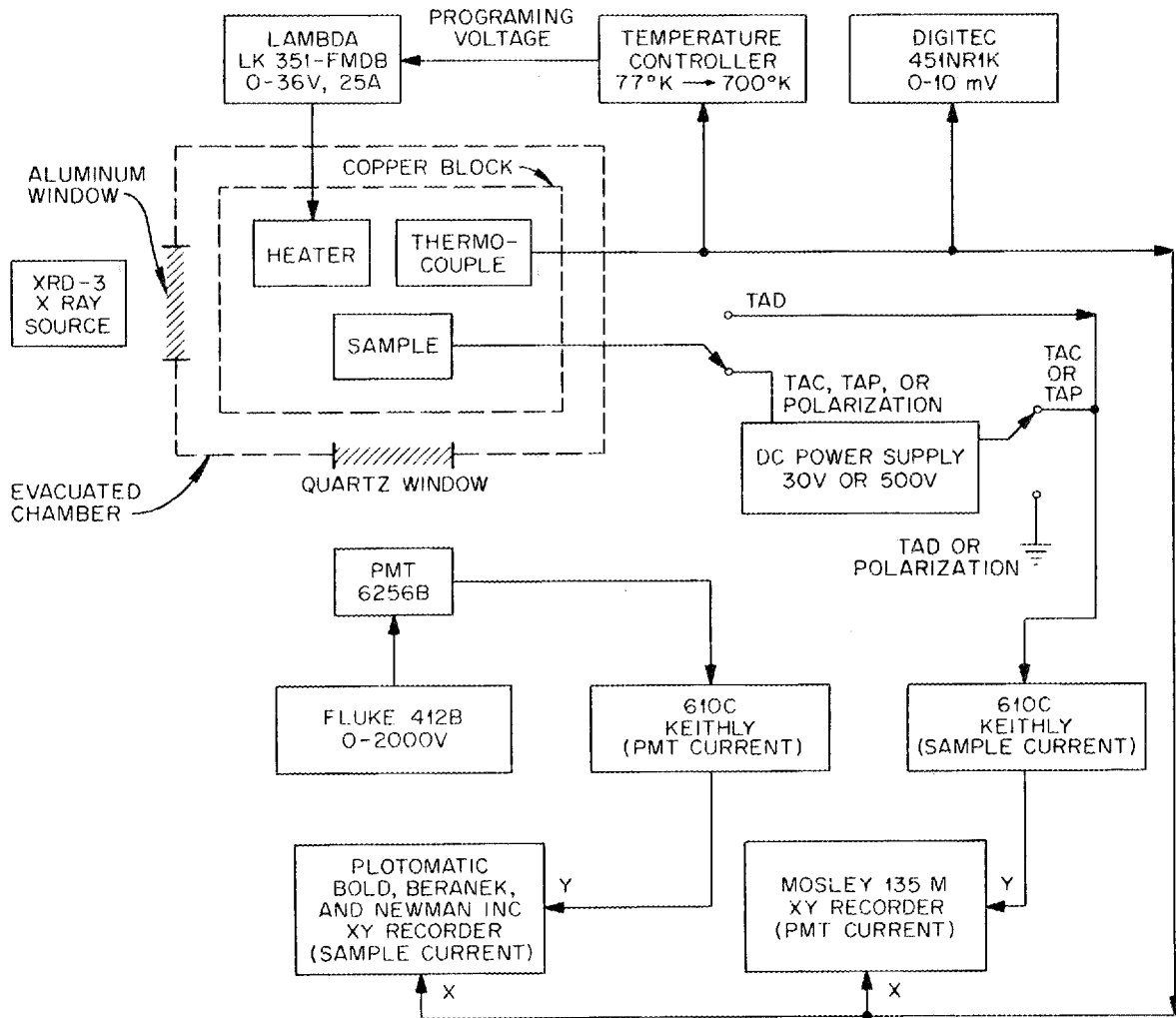


Fig. 6. Block Diagram of Electronics Used for Direct Current Experiments; For Optical Repopulation, the PMT is Replaced by a Mercury Arc Lamp.

EXPERIMENTAL RESULTS

The TAD/TAP experiments covered the range from 77°K to about 400°K. In all samples, the charge release peaks associated with the divalent impurity-vacancy dipoles occurred in the range from 200°K to 250°K. This agrees with the findings of Laj and Berge.²⁰ In all experiments, the TAP curves and the TAD curves are essentially indistinguishable and give just the comparative results expected from Eq. (31). We can therefore conclude that no large anomalies exist in the susceptibility temperature dependence of these samples within the temperature range observed.

Annealed Samples

As an annealing procedure all samples were first heated to 700°K and quenched rapidly to room temperature. Each sample then showed TAD/TAP charge release peaks with $T_m = 220^\circ\text{K}$ at a temperature scan of $0.5^\circ\text{K sec}^{-1}$. The TAD curve for a freshly annealed sample of LiF:Mg is shown as the solid line in Fig. 7. The TAD/TAP curves for annealed LiF(UV) and TLD-100 both have the same shape as for LiF:Mg. Using the whole curve analysis indicated in Eq. (28) we found for all samples a rate function $W(T)$, well described over the entire data range by the rate parameters $E_a = 0.44 \pm 0.03$ eV and $W_0 = 10^{8.5 \pm 1.5} \text{ sec}^{-1}$. The susceptibility is large; the 130-ppm LiF:Mg samples, for example, give a TAD charge release of $3 \times 10^{-10} \text{ C cm}^{-2}$ at an applied polarizing voltage of 100 volts across a 1-mm sample. The TLD-100 TAD and TAP signals are approximately the same size. The

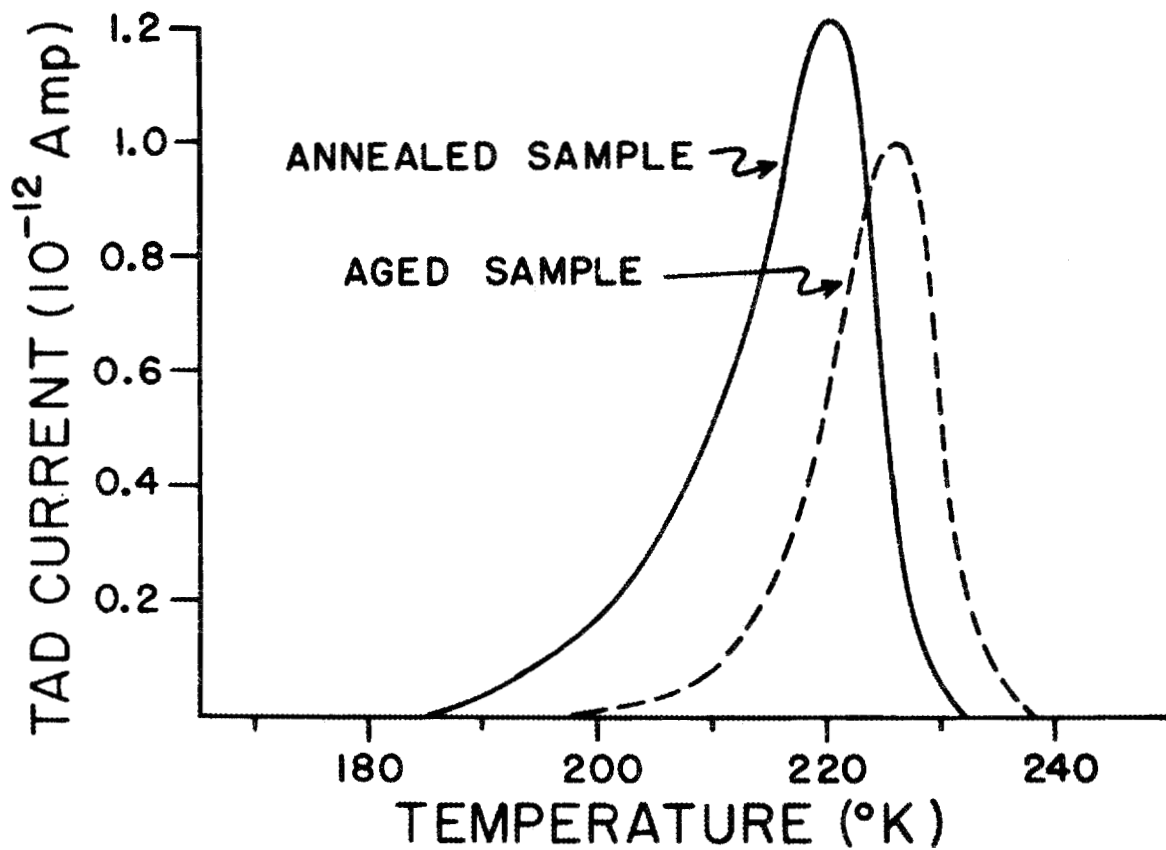


Fig. 7. Shown on the Same Plot are the .44 eV Feature (Solid Line) Ascribed to Simple Impurity-Vacancy Dipole Relaxation and the .86 eV Feature (Dotted Line) Thought to Result from Relaxation Subsequent to Dipole Aggregation.

LiF(UV) TAD/TAD peaks are somewhat less than an order of magnitude smaller. This agrees with the 10-ppm divalent ion concentration estimated from the NMR work on the LiF(UV) samples.

If we assume a Lorentz local field model for the impurity-vacancy polarization in LiF, then the susceptibility of the 130-ppm LiF:Mg is

$$\chi = 1.9 \times 10^{-11} \text{ (mks)} = 0.17 \text{ (cgs)}. \quad (37)$$

Since the dipole complex is a part of the LiF lattice, the Lorentz field may be of doubtful applicability. If only the average internal field contributes to the polarization, then the susceptibility is a factor of approximately 3.5 larger than quoted above. In any event, this polarization corresponds to an increase of the dielectric constant of the LiF:Mg sample from the nominal "pure" value of 9.0 to a value of 16.4.

The above value for the susceptibility and Eq. (7) can be used to estimate the rms vacancy-ion distance, $d^2 = p^2/e^2$. The effective polarizing temperature for either TAP or TAD is estimated sufficiently well for our purposes by $T_m = 220^\circ\text{K}$. As a most conservative approach we take $\Delta = 1$, and we take $N_0 = 10^{19} \text{ cm}^{-3}$. Then even the relatively small Lorentz local field susceptibility of Eq. (39) gives

$$\langle d^2 \rangle^{\frac{1}{2}} \geq 4.5 \times 10^{-8} \text{ cm} \quad (38)$$

We note that this value is approximately equal to the LiF f.c.c. lattice constant. The least conservative estimate is to use the average field, rather than Lorentz field, susceptibility and to take the geometrical

factor to be $\Delta = 1/3$. We then find

$$\langle d^2 \rangle^{\frac{1}{2}} \leq 14 \times 10^{-8} \text{ cm}, \quad (39)$$

and conclude that the rms divalent ion vacancy distance is between one and three lattice constants.

Aggregation Effects

As we allowed our TLD-100 and LiF:Mg samples to age for several weeks, however, we began to observe that the line shape changed in an interesting manner. The susceptibility decreased with aging and the TAP/TAD curves developed a growing high-temperature shoulder. The shoulder became increasingly well resolved, and ultimately complete conversion was observed with the formation of a single peak occurring at 226°K . The aged TAD curve for LiF:Mg is shown as the dashed line in Fig. 7. We presume this to be an aggregation¹⁴ effect. In the relatively dilute dipole LiF(UV) samples, no such effects could be detected.

The effect also was reversible; upon heating the sample to a high temperature and rapidly cooling it, the original shape and 220°K temperature maximum returned.

The TAD curves for the high divalent concentration samples after complete conversion have the following properties. First, when analyzed according to Eq. (28), we find a well-defined single activation energy behavior, $E_a = 0.86 \pm .03 \text{ eV}$ and $W_0 = 10^{19 \pm 1.5} \text{ sec}^{-1}$. Also, using the mean breadth expression in Eq. (18), we find that the rate at 226°K for the aggregated dipole TAD peak is just twice as large as the rate at

220°K for the annealed sample TAD peak. Since the rate doubling temperature interval of the annealed sample is about 6°K in this temperature range, both curves actually have almost equal values of $W(T)$.

Radiation Induced Effects

We have described previously²⁴ RITAD experiments in which we observe electronic state polarization signals. We observed a strong RITAD effect, which we associate with the impurity vacancy dipoles, at 220°K in the TLD-100 and in the LiF:Mg; the effect was present, but was very weak in the LiF(UV). Although it had the same peak temperature as did the .44-eV feature seen in these samples using TAP/TAD, its associated shape parameters were $E_a = .62 \pm .03$ eV and $W_0 = 10^{13.5 \pm 1}$ sec⁻¹. The radiation response of the impurity-vacancy dipoles is quite large. With a 5×10^3 Vcm⁻¹ field the polarization is approximately 10^{-13} C cm⁻² R⁻¹. This is somewhat greater than the radioelectret response reported by Murphy et al.²³ for Teflon.

DISCUSSION AND CONCLUSIONS

A summary of our results, together with those of Wagner,²⁵ Laj and Berge,²⁰ and Grant²⁶ is given in Table 1. It seems clear that the 220°K, .44-eV feature seen by both TAP and TAD is due to a simple dipolar reorientation effect. The dipole is formed by a Mg⁺⁺ ion and its associated cation vacancy. This mechanism is adequately described in the article by Bucci and Fieschi.¹⁸ Recent studies by Wagner and

Table 1. Summary of Impurity Ion Associated Effects in Doped and Undoped Lithium Fluoride in the Temperature Regime 200°K→250°K.

Experiment	Sample	T_m (°K)	E_a (eV)	W_0 (sec ⁻¹)
TAP, TAD	LiF:Mg	220	.44 ± .03	$10^{8.5 \pm 1.5}$
	TLD-100			
	LiF(UV)			
TAP, TAD	LiF:Mg	226	.86 ± .03	$10^{19 \pm 1.5}$
	TLD-100			
RTAD	LiF:Mg	220	.62 ± .03	$10^{13.5 \pm 1}$
	TLD-100			
	LiF(UV)(?)			
NMR data (Wagner ²⁵)	LiF:Mg		.43	
dielectric loss data (Grant ²⁶)	LiF:Mg		.75	$10^{14.5 \pm 1}$
TAD (Laj and Berge ²⁰)		217	.64	$10^{13.1}$

*Annealed and quenched

**Aged

Mascarhenas³¹ on rare earth-doped CaF_2 show that one may expect only small activation energy differences depending upon which particular impurity ion is present in the complex. Consequently, in the TLD-100 and the LiF(UV) samples, the dipole system may be formed of many different divalent ion-vacancy complexes.

The activation energy of annealed samples given in Table 1 is in good agreement with that measured by Wagner²⁵ in NMR experiments for the same sample batch of LiF(UV) and LiF:Mg. He obtained shape parameters of $.41 \pm .03$ eV and $.45 \pm .03$ eV. Our value of $W_0 = 10^{8.5 \pm 1.5}$ is much smaller than that given in a physical interpretation of an "attempt frequency" for diffusion. One expects a value closer to 10^{11} or 10^{12} sec^{-1} for the latter. In dipolar reorientation the vacancy must make a number of diffusion jumps to accomplish relaxation of the dipole. A simple diffusive calculation shows that W_0 should be related to the mean vacancy jump attempt time, T_j , by

$$W_0 = (\Delta\theta)^2 / 2T_j, \quad (40)$$

where $\Delta\theta$ is the rms angular jump of the vacancy about the divalent ion, defined as the angular jump distance divided by the nearest neighbor distance, i.e., assuming diffusion to be dominated by nearest neighbor jumps. We thus see that our measured "attempt frequency" is therefore $10^{11.5 \pm 1.5}$.

The 226°K , .86-eV TAP/TAD effect is apparently the formation of a stable state due to dipole aggregation in samples containing relatively

high impurity levels. Several investigators have studied the growth of dipole complexes^{29,30} in other materials. Capelletti and Fieschi³² have recently observed the growth of a second TAD peak in KCl:Eu, in which the two TAD curves were simultaneously resolvable. We believe our study may be the first recognition of similar effects in LiF:Mg. It is likely, though, that the feature seen in the LiF:Mg material at $E_a = .65$ eV by Laj and Berge²⁰ and at a value of $E_a = .75$ eV by Grant²⁶ is also the result of aggregation.

We see that our results for freshly annealed samples agree with those of Wagner²⁵ for similar samples. Upon aging for many weeks, however, our TAD/TAP peaks the samples convert into apparent kinetic behavior much closer to that measured by Laj and Berge²⁰ or by Grant.²⁶

A very interesting feature of the various experimental results can be seen in Table 1. In all cases, although the apparent activation energies change, the ratio of the activation energy to the logarithm of W_0 is essentially constant. This is just the relationship expected, as indicated in Eqs. (35) and (36), in a system where E_a becomes slightly temperature dependent. We speculate that aggregation effects cause this temperature dependence, but that $E_a(T)$ for the aged samples is not very different from E_a for the annealed samples. In such a case, we expect the "characteristic" parameter to be the peak temperature, assuming a constant heating rate. That the apparent E_a and W_0 are really E^* and W_0^* as defined in Eqs. (33) and (34) is the reason we are not disturbed by what appears to be an unreasonably large pre-exponential factor. The

values of $E_a = .86$ eV and $W_0 = 10$,¹⁹ then, are reproducible and strongly suggest some dipole-dipole interaction is taking place, although our simple model does not permit its calculation a priori. The magnitude of this dipole-dipole interaction depends upon the individual dipolar susceptibility, which varies inversely with temperature. Thus we expect that the aggregated and nonaggregated systems behave very similarly at high temperatures, where the dipole-dipole interaction is small, but slightly differently at low temperatures, where the temperature dependent interaction leads to perturbations in E_a and W_0 . It is well documented that the TL spectrum of Mg doped lithium fluoride is a function of pre-irradiation annealing procedures³³--this, too, is apparently a result of the formation of ionic clusters, most likely of the M_g^{++} ion. This ion is known to be present in most dosimetric grades of lithium fluoride.

The large susceptibility of this system gives a minimum rms ion-vacancy distance [Eq. (38)] greater than the fcc lattice constant. Thus there is substantial lattice polarization within the system from the nearest neighbor LiF pairs. Therefore, one can hardly justify use of the Lorentz field as the polarizing field sensed by the complex. The alternative is that the complex polarizes in the average field. We therefore conclude that the value $\langle d^2 \rangle^{\frac{1}{2}} = 14A^{\circ}$ given in Eq. (39) is the more realistic estimate. This large value is not inconsistent with models and measurements which put the average vacancy position between nearest and next nearest neighbors. The polarizability, which we have studied,

measures the second moment of the distance distribution, d^2 . A large value of d^2 implies only that the wings of the distribution are not sharply truncated.

We believe that our RITAD effect with $T_m = 220^\circ\text{K}$, $E_a = .62$ eV, and $W_0 = 10^{13.5} \text{ sec}^{-1}$ is essentially the same as TAD, but where polarization in the presence of the applied field at low temperature (app. 80°K) has occurred due to local heating of the ionic environment by "hot" radiation induced electrons and holes. We can view this as a normal radioelectret effect on the impurity-vacancy dipole system. We suspect these charge carriers become trapped in the immediate vicinity of the polarized ionic dipoles and cite recent investigations³⁴ which suggest and verify this hypothesis. This leads to an attendant charge carrier-ionic dipole interaction which produces a temperature dependence of the activation energy, which causes a shift in the curve parameters W_0^* and E_a^* but leaves the peak temperature relatively unperturbed.

To conclude, we have performed TAP, TAD, and RITAD experiments on LiF samples with varying divalent ion concentrations. We have observed thermally activated reorientation of impurity-vacancy complexes. The TAD/TAP susceptibilities measured in these samples imply an rms dipole length between 4.5 and 14\AA . It appears that the larger value more likely represents the actual situation.

Depending upon sample history we find three different sets of rate parameters. Freshly annealed samples give $E_a = 0.44 \pm 0.3$ eV and $\log W_0 = 8.5 \pm 1.5$. These parameters agree with those determined from NMR

relaxation experiments.²⁵ As the samples age, the TAP/TAD curves in heavily doped samples become converted to a much narrower shape, although the temperature of the peak maximum shifts only slightly. The aged sample curve is characterized by $E_a = .86 \pm .03$ eV and $\log_{10} W_0 = 19 \pm 1.5$. We suspect that these aggregation effects have occurred in other experiments as well, and account for the large apparent activation energies observed by Grant²⁶ and Laj and Berge²⁰ in the LiF system. These dipoles also show RITAD response, which occurred in all samples at 220°K, and for which we find $E_a = 0.62 \pm .03$ eV and $\log_{10} W_0 = 13.5 \pm 1$. This variation in apparent kinetic behavior can be consistently interpreted as dipole-dipole or dipole-trapped-charge interactions which slightly alter the temperature dependence of the reorientation activation energy.

CHAPTER III

OBSERVATION OF A RADIATION-INDUCED THERMALLY ACTIVATED
DEPOLARIZATION IN LITHIUM FLUORIDE

We have observed that an intense stable electrical polarization can be induced when a sample of high purity LiF is subjected to a polarizing field during simultaneous X-ray irradiation. The effect is readily detected after irradiation by shorting the polarizing electrodes through an ammeter, heating the sample at an approximately constant rate, and recording, as a function of temperature, the thermally activated current generated by sample depolarization. We also observe that, after initial irradiation of relatively high-purity samples, the dominant charge release peak can be optically regenerated. Before irradiation, the samples exhibit some weak electret activity from ionic thermocurrent (ITC) states¹⁸ with characteristic activation temperatures around 220°K; this is due to trace concentrations of divalent ion-vacancy complexes, but at our exposure levels, radiation damage induces no other detectable purely thermal-electret activity as has been observed in certain other dielectrics.³⁵⁻³⁸ Sample irradiation does produce, from these ITC states, a small radioelectret effect similar to that observed²³ in Teflon and carnauba wax, both of which form strong thermal electrets. This Letter, however, is mainly to report much stronger and different effects observed below 200°K; these intense polarizations clearly arise from very different physical origins than the ITC, radioelectret, or electret decay^{22,39} phenomena previously studied. Consequently, we subsequently refer to all these

effects by the general description of a "thermally activated depolarization" (TAD) or "radiation-induced thermally activated depolarization" (RITAD).

An example of the RITAD peaks is shown in Fig. 8 for the temperature range from 85°K to 240°K from a 1-x-1-x 0.075-cm³ sample of Harshaw uv optical quality, UV-H63A, high-purity LiF [LiF (UV)]. The dotted line in Fig. 8 shows the thermoluminescence (TL) glow curve measured simultaneously with the RITAD curve. For Fig. 8, the exposure is about 100R, and the polarizing field about 500 V/cm in the sample. The temperature scan corresponds to constant heater power and varies from about 0.5°K sec⁻¹ at the higher temperatures to about 0.75°K sec⁻¹ at the lower temperatures. We measure approximately one electron of electrode compensation charge for each 10⁴ keV of X-ray energy absorbed by the LiF. This radio susceptibility is about 10⁵ times stronger than the radioelectret polarization of carnauba wax.²³ We have, as yet, acquired insufficient detailed data on these effects to give a fully quantitative description of much of the behavior. We believe, however, that this new phenomenon has enough practical potential to warrant this chapter outlining only our semiquantitative descriptions and qualitative results. The apparatus is essentially the same as described previously for TL studies,¹³ but modified for attachment of sample electrodes. A more detailed discussion of our experimental procedures, RITAD curve analysis, sample treatments, etc., will be published subsequently. In the following discussion, because of its descriptive purposes, the temperatures quoted are simply the sample mounting block

ORNL-DWG 72-12975

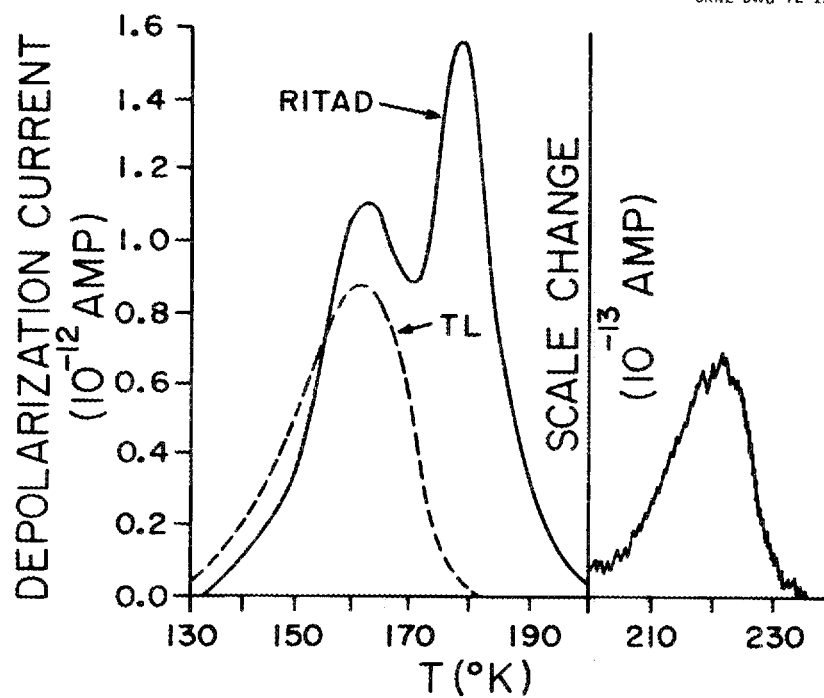


Fig. 8. The Solid Curve Shows the RITAD Current in a Sample of High-Purity Optical Quality LiF. The dashed curve shows simultaneously recorded thermoluminescence emission.

temperatures. Some sample mounting procedures may cause the actual sample temperature to lag behind the block temperature and to be as much as 10°K cooler at the lower temperatures.

Although the central $\sim 180^{\circ}\text{K}$ peak shown in Fig. 8 displays the most striking RITAD properties, the overall RITAD behavior requires complicated verbal description, and so we begin by discussing other preliminary experiments. First, prior to laboratory X-ray exposure, one can measure ionic thermocurrents by applying a polarizing field at about room temperature, cooling the sample to freeze in any impurity electret state polarization, and then performing a TAD experiment. The inverse experiment is thermally activated polarization (TAP); one starts with a cold, unpolarized sample and heats in the presence of an applied field to measure the polarization currents. In both TAD and TAP one observes charge release peaks at the same temperature and associated with the highest-temperature (220°K) RITAD peak shown in Fig. 8. If we perform TAD/TAP ionic thermocurrent experiments with divalent-ion-doped samples of LiF, either thermoluminescence dosimetry grade [LiF-TLD(100)], or samples doped to 130 ppm with magnesium, LiF:Mg, we observe qualitatively similar behavior of the 220°K TAP/TAD features; the intensity, however, is very much greater than in the LiF(UV) samples. We apply a whole curve analysis, such as described by Bucci and Fieschi¹⁸ which we can also modify for TAP effects, to the polarization curves and thereby extract activation energies and frequency factors describing the 220°K features. We assume here a rate W for depolarization; $W(T) = s \exp(-E/kT)$, where E may itself be temperature

dependent.^{14,40} In general the peaks seem to be well described by first-order kinetics, each peak having a definite activation energy E . We feel that the activation energy is useful for labeling a particular peak and, together with the rate parameter s , gives some indication of the physical processes responsible for the observed phenomena. For present purposes it suffices to say that the 220°K features are ITC states associated with impurity divalent ion-vacancy dipolar complexes; their RITAD activity seems to be the radioelectret polarization of these existing dipoles and, for annealed samples aged at room temperature for several weeks, the measured ITC rate parameters are $E = 0.44 \pm 0.02$ eV and $\log_{10}(s) = 9 \pm 1.5$.

A second experiment is the measurement of radiation-induced thermally activated conductivity (TAC); the sample is irradiated at low temperatures to produce trapped electrons and holes. One then applies an electric field, heats the sample, and monitors the conductivity to record the TAC curve resulting from the release of the charge carriers into mobile states prior to their recombination. This phenomenon is also called thermally stimulated conductivity by some investigators. In a TAC experiment one also observes TAP effects, as described previously, from dipolar entities; the two can be differentiated because the TAP effects can also be identified in an ionic thermocurrent TAD experiment. When a radiation-induced TAC run is performed on any of our samples we observe activity associated with the low-temperature TL peak ($\sim 162^\circ\text{K}$) shown in Fig. 8, as well as already measured TAP activity from the 220°K features. Simultaneous TL measurements show near-uv emission in a very strong glow peak correlated

with the 162°K TAC peak and show that this TL is not repopulated by subsequent uv irradiation. The activation rate parameters for either the TAC or TL peak at 162°K are $E = 0.25 \pm 0.02$ eV and $\log_{10}(s) = 7 \pm 1$. All these features correspond with previous experiments at this lab^{13,14} where the TL peak was associated with the activated mobility of the self-trapped hole V_k center. It therefore appears that the RITAD effect shown in Fig. 8 results from the dipole moment generated by net charge separation of the V_k center hole and its charge-compensating associated trapped electron when irradiation is carried out in a polarizing field. The V_k center 0.25-eV TAC peak can be observed in all our specimens, LiF(UV), LiF-TLD(100), and LiF:Mg. When a previously unirradiated crystal is exposed at liquid- N_2 temperature to optical illumination from a 75-W mercury arc through quartz optics, we can observe no optical generation of TAC, TL, TAD, or TAP effects.

Finally, we can discuss the RITAD behavior specifically; when our LiF(UV) samples are irradiated with X-rays in the presence of a polarizing voltage of 500 V, the RITAD curve shown in Fig. 8 results. In the LiF:Mg and the LiF-TLD(100) samples the 220°K RITAD features, which we identify as radioelectret polarization of pre-existing ITC states, are typically stronger by more than a factor of 10 than those shown in Fig. 8 for the LiF(UV) sample. On the other hand, in LiF(UV) the central RITAD peak at $\sim 180^{\circ}\text{K}$ is much more intense than in the doped samples. Because we can measure the overlapping V_k center 0.25 eV peak in a TAC experiment, its contribution can easily be subtracted for good analysis of the central

180°K RITAD peak, which is characterized by $E = 0.34 \pm 0.05$ eV and $\log_{10}(s) = 8.5 \pm 1.5$. The most interesting features of the 0.34 eV peak in LiF(UV) are the following: (1) It cannot be detected in TAP, or regenerated, as can an electret or the ionic thermocurrent features at 220°K, by a high-temperature polarizing process once it has been thermally depolarized. (2) We have not been able to detect the 0.34-eV RITAD peak in a TAC experiment nor to observe any correlated TL activity; thus this strong RITAD effect does not appear to be a radioelectret effect, in the sense of the usual meaning of the term. (3) In contrast to the $V_k 0.25$ eV peak and 220°K ITC peaks, however, the strong 0.34 eV RITAD peak in LiF(UV) can be optically regenerated. After X-raying and thermal depolarization, the sample can again be thermal depolarization, the sample can again be cooled and the 0.34 eV RITAD peak regenerated by applying a polarizing voltage simultaneous with sample illumination through quartz optics from a small Hg arc source. A comparison of the direct RITAD and optically regenerated RITAD curves is shown in Fig. 9. We note that the optically regenerated RITAD peak appears to shift to higher temperature by about 10°K with respect to the direct 0.34 eV peak. However this may be an experimental artifact, since the whole curve analysis shows that the optically regenerated curve has rate parameters of $E = 0.37 \pm 0.04$ eV and $\log_{10}(s) = 9 \pm 1$, both of which are within our experimental error of those for the direct RITAD 0.34 eV peak. With a soft glass filter between the sample and the optical source to absorb radiation with wavelengths less than about 3000Å, no optical regeneration occurs.

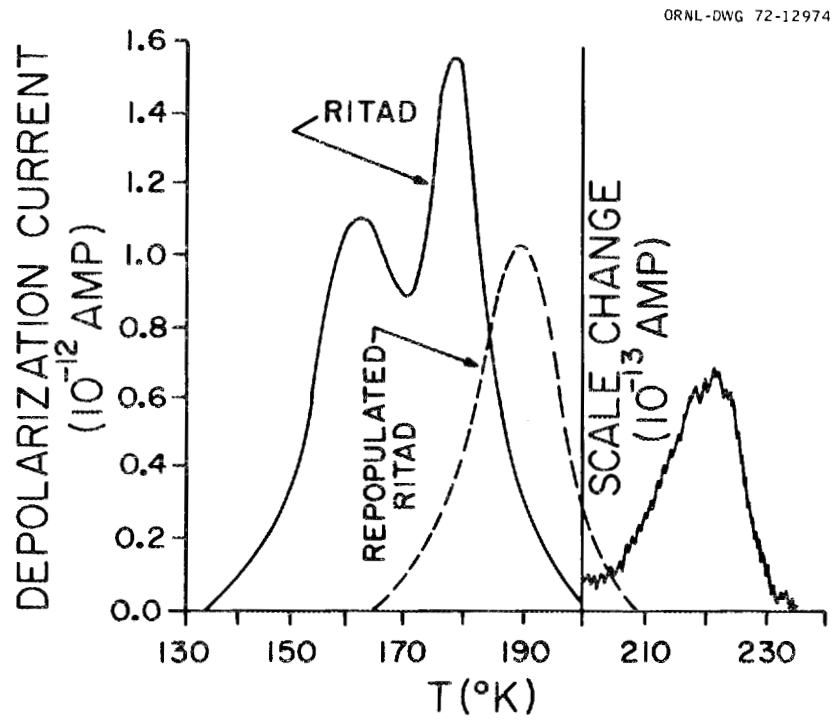


Fig. 9. The Solid Curve Shows the LiF(UV) Direct RITAD Effect and the Dashed Curve Shows Its Subsequent Optical Regeneration.

In the LiF:Mg and the TLD(100) samples, both the 0.34-eV RITAD peak and its optical repopulation are heavily suppressed with respect to those observed in the undoped LiF(UV) samples. It is clear that the strong 0.34 eV RITAD peak in LiF(UV) is extremely sensitive to sample impurity content.

Our preliminary observations show that the RITAD effects can be strongly supralinear in absorbed dose; at least up to about 10^3 rad, our initial rough experiments indicate that the total thermal charge release may scale approximately as the cube of the X-ray exposure. We also observe that the signal-to-noise ratio in measuring RITAD peaks is perhaps a bit better than that in simultaneous measurement of TL peaks. Optical considerations limit sample size for increasing sensitivity in TL dosimetry, but there are no such limitations on measuring RITAD. Because RITAD effects do not intrinsically require conductive electrical continuity or good optical quality of the sample, they can be measured for sintered or extruded samples, or for RITAD materials extruded as a suspension in a matrix. Since at least some RITAD peaks can be regenerated optically, irradiation received at higher temperatures in the absence of a polarizing field can be measured at a later time using optically regenerated RITAD. Because of the considerations outlined above, it would seem that these radiation-induced polarization phenomena may provide a wealth of possibilities for sensitive dosimetric techniques not possible with other radiation-induced phenomena.

Added note - Since submission of this manuscript, further experiments have revealed a variety of RITAD effects in other dielectrics. In CaF_2 , for example, we can observe a RITAD phenomenon having at least 10^3 greater charge release per rad than for the $\text{LiF}(\text{UV})$ described above.

CHAPTER IV

CONCLUSIONS

In our first chapter, we describe results of our test of the simple trapped carrier-free carrier recombination model normally used to describe TL and TAC effects. We analytically derive an exact correlation expression for TL and TAC effects which implies, in its inability to describe experimental results, the nonvalidity of the model. An examination of the manner in which the model predictions disagree with our results indicates that a suitable additional model hypothesis, the existence of a significant degree of spatial correlation between trapped carriers and recombination centers, will bring the model into agreement with the experiment.

In Chapter II we describe our experiments on LiF crystals doped to various impurity levels and with different thermal histories. We conclude that consistent changes in activation energy and rate parameters with doping level and sample treatment are likely due to the activation energy E_a and rate parameter W_0 developing a temperature dependence as the divalent impurity-vacancy dipoles aggregate. Chapter II is important to this thesis chiefly in two ways. Firstly, our results here enable us to subtract the TAP contribution from dipolar polarization effects as we collect data in a TAC experiment. Secondly, an important unforeseen result of these analyses is our ability to reconcile earlier NMR, TAD, and dielectric loss results that show radically different values for the activation energy and rate parameter.

Chapter III describes the RITAD experiment and our observations of this effect in doped LiF. We conclude that this effect, due to its high signal-to-noise ratio and the fact that its intensity may be remeasured after optical repopulation, may have useful application in the area of radiation dosimetry. The RITAD effects are shown, by reference to those effects investigated in Chapters I and II, to have perhaps several origins. The .34 eV RITAD effect appears to be closely related to our correlated 160°K TL/TAC peaks assumed to be related to V_k center recombination. It may be that here we observe a polarization of the electric dipoles formed by the V_k center and its associated electron. Our higher .62 eV RITAD peak is apparently correlated with our 220°K impurity-vacancy dipole polarization effect, and may indicate an interaction between the "ionic" electric dipoles and electron or hole charge carriers trapped nearby. This could lead to temperature-dependent shape parameters which would, as described in Chapter II with reference to dipole aggregation effects, leave the peak temperature relatively unchanged.

We have shown that the TAP effect (Chapter II) can significantly mask or cause the misinterpretation of data obtained in an experiment designed to measure TAC (Chapter I). It is also significant that the TAC signals (Chapter I) are observed in the same temperature range as is the RITAD effect (Chapter III). This suggests these effects may have similar origins; it may be that RITAD is a TAC effect due to charge carriers trapped in the neighborhood of, and consequently within the electric field of, those impurity-vacancy dipoles responsible for the TAD/TAP effects described in Chapter II. Those aggregation effects described in Chapter II suggest

that at least some impurity states may in highly doped samples exhibit strong spatial correlations. This may be significant with regard to TL/TAC results in Chapter I which also suggest spatial correlations.

These spatially correlated trapped carriers and TL-active recombination centers discussed in Chapter I might be a result of the concentration of each entity along damage tracks in the material, or instead an increased probability of finding these entities near dipoles or dipole aggregates. This suggests that future systematic studies of very lightly doped samples, where dipole aggregation would not be so pronounced, are in order.

Nor do the experiments of Chapter I positively resolve whether failure of the relation $\eta \neq \eta(T)$ or of the equation $\partial_t f/M+f = -\gamma n_c$ is responsible for failure of the simple model. If one uses a population sensitive technique, such as ESR or optical absorption to monitor $f(t)$ or $n(t)$ directly, rather than relying on monitoring $\phi = -\eta \partial_t f$, one might be able to do a correlation check between these techniques and TAC, and to derive an accompanying correlation expression with the η dependence removed. An experiment of this type could determine which of the above model equations is violated. Should η be proven to be constant, the theoretical incorporation of trapped carrier-recombination center spatial correlation would be a possible modification to the general model. Experiments on TAC/TL correlations as functions of sample treatment, accumulated dose, and applied field might also be of value, especially in light of the well known supralinear TL response of LiF with increasing dose.

A logical extension of the experiments discussed in Chapter II is a careful study of the decay of the .44 eV feature and the growth of the

.86 eV feature as functions of sample composition and of time and temperature so as to elucidate the aggregation kinetics. Also, if it is possible to observe a RITAD effect due to charge carriers trapped near impurity vacancy dipoles, might not the TAP/TAD shape parameters and peaking temperatures be influenced by these nearby trapped carriers? TAP/TAD experiments subsequent to irradiation to determine if this effect exists should also be carried out. At high doping levels, is ferroelectric domain behavior observed? Presumably in this experiment we observed temperature dependent TAP/TAD shape parameters resulting from aggregations of like impurities. Cook and Dryden²⁹ observed trimer formation in alkali halides. Would, in a sample doped with two impurities, we see effects resulting from stable dipole aggregates of unlike impurities?

Regarding Chapter III, a correlation of the RITAD effect with TL, TAC, or other electron-hole related effects, and with impurity-vacancy dipole derived effects such as TAP and TAD would be useful. The RITAD effect appeared to be supralinear with irradiation--a study of RITAD vs. dose and vs. applied field would be interesting. Also, does this effect exhibit any variation in sensitivity as a function of irradiation temperature, assuming the irradiation is performed in all cases well below the read-out temperature? Finally, a study should be made of RITAD repopulation as functions of irradiation wavelength and of time, correlated with measurements of RITAD repopulation intensity as a function of the concentration of carriers remaining trapped at higher activation energies. These experiments would determine if RITAD repopulation appears to be brought about in a manner similar to repopulation of TL and TAC.

APPENDIX I

ON THE RELATION BETWEEN THE EXPERIMENTALLY
DETERMINED PRE-EXPONENTIAL FACTOR W_0 AND THE
MICROSCOPIC VACANCY JUMP TIME, τ_0

One notes in Chapter II, Table 1, that the experimentally determined value of the pre-exponential W_0 , interpreted as an effective attempt frequency for dipole rotation at infinite temperature, is $10^{8.5 \pm 1.5} \text{ sec}^{-1}$. Most other measurements where a simple first-order kinetics model of this sort has been used (e.g., thermoluminescence) indicate that a value of 10^{11} or 10^{12} sec^{-1} would be anticipated. The reason for this difference may be explained by the argument that whereas thermoluminescence is sensitive to the actual jump time for charge carrier diffusion, experiments of the TAP/TAD genre are sensitive to average times for dipole rotation, i.e., to the diffusion time of a trapped vacancy completely about an associated impurity ion. A classical diffusion approximation relating dipole rotation to vacancy diffusion should give us a rough idea of the ratio between these characteristic times.

One may compare the rotation of the dipole moment to that of the axis of a rigid sphere of radius a in a viscous medium. Thus, we assume a diffusion equation

$$\frac{\partial \psi(\Omega, t)}{\partial t} = \frac{D}{a} \nabla^2 \psi(\Omega, t)$$

where ∇^2 is the angular Laplacian operator, D is the diffusion constant for rotation (for a rigid sphere in a medium of viscosity η , D is $\frac{kT}{8\pi\eta a}$ by Stoke's law), and $\psi(\Omega, t)$ is the probability of finding the axis in the direction Ω at the time t .

Seeking a solution of the diffusion equation as an expansion in spherical harmonics, we take

$$\psi(\Omega, t) = \sum_{\ell} \sum_{m} c_{\ell}^m(t) Y_{\ell}^m(\Omega).$$

Substitution into the diffusion equation gives

$$\frac{dc_{\ell}^m}{dt} = -\frac{D}{a^2} \ell(\ell+1) c_{\ell}^m$$

which leads to

$$c_{\ell}^m(t) = c_{\ell}^m(0) e^{-t/\tau}$$

where

$$\tau = \left[\frac{D}{a^2} \ell(\ell+1) \right]^{-1}$$

is interpreted as being the observed characteristic dipole relaxation time.

Applying the initial condition

$$\begin{aligned} \psi(\Omega, 0) &= \delta(\Omega - \Omega_0) \\ &= \sum_{\ell} \sum_{m} c_{\ell}^m(0) Y_{\ell}^m(\Omega) \end{aligned}$$

together with the expansion for the delta function in spherical harmonics

$$\delta(\Omega - \Omega_0) = \sum_{\substack{l \\ m}} Y_l^m(\Omega_0) Y_l^m(\Omega)$$

leads to the identification

$$\psi(\Omega, 0) = \sum_{\substack{l \\ m}} Y_l^m(\Omega) e^{-t/\tau}.$$

In looking at the change in polarization of a given material one is concerned with the projection of the microscopic dipole moment onto some preferred axis. The relevant quantity is $\langle \cos\theta \rangle$, where θ is the average value of the angle between the dipole moment and some arbitrary direction in space.

Now

$$\begin{aligned} \langle \cos\theta \rangle &= \int_{\Omega} \cos\theta \psi(\Omega) d\Omega \\ &= \int_{\theta} \int_{\varphi} \cos\theta \sum_{\substack{l \\ m}} Y_l^m(\Omega_0) Y_l^m(\Omega) e^{-t/\tau} d(\cos\theta) d\theta \\ &= e^{-t/\tau} \int_{\theta} \cos\theta \sum_{\substack{l \\ m}} Y_l^m(\Omega_0) Y_l^m(\Omega) d(\cos\theta) d\theta \end{aligned}$$

but since $\cos\theta \propto Y_1^0$ and the integrand integrates to zero for all $m \neq 0$, $l \neq 1$, we get

$$\langle \cos\theta \rangle = (\text{const.}) Y_1^0(\Omega_0) e^{-t/\tau}$$

thus verifying the identification of τ as the observed dipole relaxation time, and indicating that $l = 1$ in the equation for τ .

D may be approximated by

$$D \approx \frac{\text{jump length}^2}{4\tau_o}$$

$$\approx \frac{\theta_j^2 a^2}{4\tau_o}$$

where τ_o is the characteristic vacancy jump time and θ_j is some characteristic jump angle.

Substitution in the equation for τ gives

$$\tau = \frac{4 a^2 \tau_o}{\theta_j^2 a^2 l(l+1)} = \frac{2\tau_o}{\theta_j^2} .$$

The approximation $\theta_j \approx 30^\circ$, for example, yields

$$\tau = \frac{2\tau_o}{(\pi/6)^2} = 7.3\tau_o .$$

The upper limit of our experimental determination of W_o is 10^{10} sec^{-1} . The above computation indicates that our measured attempt frequency for dipole rotation should be lower than the microscopic jump rate for vacancy diffusion by about a factor of 10, thus indicating our estimate of the microscopic jump rate to be a "reasonable" value of around 10^{11} sec^{-1} .

APPENDIX II

METHOD OF DATA ANALYSIS USED TO OBTAIN E_a and W_0

It was thought that an explicit description of the data analysis procedure used to obtain E_a and W_0 in Chapters II and III would be a useful appendix to this work. Equation (28) of Chapter II tells us that, for TAD,

$$W(T) = I(T) \partial_t T / \int_T^{T_2} I(T) dT$$

where $I(T)$ is the observed sample current at the temperature T , $\partial_t T$ is our experimental (linear) heating rate, and T_2 is the temperature at which the signal goes to zero on the high temperature tail. We have shown that this equation is approximately correct for the TAP effect as well, provided we take T_2 as the temperature at which the signal crosses zero.

In our data analysis procedure, we first digitize the signal manually; then, using a computer program written for this purpose, we compute $W(T)$ for the range of temperature over which we have statistically meaningful data.

We assume a rate equation of the Arrhenius form,

$$W = W_0 e^{-\beta E_a},$$

where $\beta = 1/kT$.

Plotting $\ln W(T)$ vs. β allows us to find W_0 by extrapolation to $\beta = 0$, while the slope of this plot allows us to compute E_a using the equation

$$\partial_\beta W = -W_0 E_a e^{-\beta E_a} .$$

As we point out in Chapter II, we can as an independent check of these values compute W_0 via Eq. (29) from the peak temperature T_m once E_a is known:

$$W_0 = \partial_t T E_a e^{E_a/kT} / kT_m^2 .$$

REFERENCES

1. M. Bohm and A. Scharmann, Z. Physik 225, 44 (1969).
2. M. Bohm and A. Scharmann, Phys. Stat. Sol. (a) 4, 99 (1971).
3. M. Bohm and A. Scharmann, Phys. Stat. Sol. (a) 5, 563 (1971).
4. W. A. Buckman, Thesis, University of North Carolina, 1967.
5. I. J. Saunders, J. Phys. C 2, 2181 (1969).
6. P. Kelly and P. Braunlich, Phys. Rev. B 1, 1587 (1970).
7. P. Braunlich and P. Kelly, Phys. Rev. B 1, 4, 1596 (1970).
8. P. Kelly, M. Laubitz, and P. Braunlich, Phys. Rev. B 4, 6, 1960 (1971).
9. G. W. Fabel and H. K. Henisch, Sol. St. Elect. (GB) 13, 9, 1207 (1970).
10. G. W. Fabel, Thesis, Pennsylvania State University, 1971.
11. M. L. Perlman, J. Electrochem. Soc. 119, 892 (1972).
12. J. Zimmerman, J. Phys. Chem.: Solid St. Phys. (GB) 4, 3277 (1971).
13. E. B. Podgorsak, P. R. Moran, J. R. Cameron, J. Appl. Phys. 42, 2761 (1971).
14. P. R. Moran and E. B. Podgorsak, Scientific Report C00-1105-164, United States Air Force.
15. D. E. Fields and P. R. Moran, "A Study of Thermally Activated Polarization Effects in Pure and Magnesium Doped Lithium Fluoride" (1973, to be published).
16. G. W. Stewart, Linear Least Squares Solutions, CTC-39, ed. G. W. Westley and J. A. Watts, Computing Technology Center, P. O. Box P, Oak Ridge, Tennessee, pp. 383-391 (1970).

17. S. Bozeman, private communication.
18. C. Bucci and R. Fieschi, *Phys. Rev.* 148, 2, 816 (1966).
19. S. Benci and C. Bucci, Final Scientific Report AF-EOAR-65-07, OAR, United States Air Force.
20. P. C. Laj and P. Berge, *J. Physique* 28, 821 (1967).
21. B. Gross and R. J. deMoraes, *J. Chem. Phys.* 37, 710 (1962).
22. P. V. Murphy, *J. Phys. Chem. Solids*, 24, 329 (1963).
23. P. V. Murphy, S. C. Ribeiro, F. Milanez, and R. J. deMoraes, *J. Chem. Phys.*, 38, 2400 (1963).
24. D. E. Fields and P. R. Moran, *Phys. Rev. Letters* 29, 721 (1972).
25. Jerome Wagner, University of Wisconsin, Doctoral Thesis, 1970, unpublished.
26. R. M. Grant, University of Wisconsin, Doctoral Thesis, 1965, unpublished; *J. A. P.* 37, 10, 379 (1966).
27. C. H. Haake, *J. Opt. Soc. Am.* 47, 7, 649 (1957).
28. E. B. Podgorsak, P. R. Moran, and J. R. Cameron, *Proc. Third Int. Conf. on Luminescence Dosimetry, Roskilde, Denmark; RISO* 249, 1 (1971).
29. J. S. Cooke and J. S. Dryden, *Proc. Phys. Soc.* 80, 479 (1962).
30. R. Capellitti and E. Okuno, *Proc. 142nd International Meeting of the Electrochemical Society, Division of Dielectrics and Insulators; Miami Beach, Florida; October 8-13, 1972.*
31. J. Wagner and S. Mascarhenas, to be published in *Journal of Electrochemical Society, Proc. of 142nd Meeting of Electrochemical Society, Division of Dielectrics and Insulators, Miami Beach, Florida, October 8-13, 1972.*

32. R. Capelletti and R. Fieschi, Proc. 142nd International Meeting of the Electrochemical Society, Division of Dielectrics and Insulators, Miami Beach, Florida, October 8-13, 1972.
33. D. W. Zimmerman, C. R. Rhyner, and J. R. Cameron, Health Physics 12, 525 (1966).
34. S. Unger and M. M. Pearlman, Proc. 142nd International Meeting of the Electrochemical Society, Division of Dielectrics and Insulators, Miami Beach, Florida, October 8-13, 1972.
35. W. Scislowski, Acta Phys. Pol. 7, 127 (1938).
36. J. Gomulkiewicz, Phys. Status Solidi 3, 276 (1963).
37. J. Gomulkiewicz, Acta Phys. Pol. 30, 549 (1966).
38. J. Gomulkiewicz, Acta Phys. Pol. 31, 575 (1967).
39. P. V. Murphy and S. C. Ribeiro, J. Appl. Phys. 34, 3138 (1963).
40. P. R. Moran and E. B. Podgorsak, Proceedings of the Third International Conference on Luminescence Dosimetry, Danish Atomic Energy Commission Research Establishment, Riso, Denmark, 11-14 October 1971 (unpublished).

ORNL-4850
UC-34 - Physics

INTERNAL DISTRIBUTION

- | | |
|----------------------------------------------------------------|----------------------|
| 1-3. Central Research Library | 121. W. H. Jordan |
| 4. ORNL - Y-12 Technical Library
Document Reference Section | 122. J. B. Mankin |
| 5-54. Laboratory Records Department | 123. R. D. McCulloch |
| 55. Laboratory Records, ORNL R.C. | 124. M. T. Mills |
| 56. Patent Office | 125. M. R. Patterson |
| 57-66. Mathematics Division Library | 126. M. R. Reeves |
| 67. A. A. Brooks | 127. A. H. Snell |
| 68. H. P. Carter | 128. J. G. Sullivan |
| 69. F. L. Culler | 129. D. A. Sundberg |
| 70-119. D. E. Fields | 130. A. M. Weinberg |
| 120. R. F. Hibbs | 131. A. Zucker |

EXTERNAL DISTRIBUTION

132. L. E. Barroilhet, Physics Department, University of Wisconsin, Madison, Wisconsin 53706
133. Larry Dewerd, Department of Metallurgy, Roberts Hall, University of Washington, Seattle, Washington 98105
134. G. Fuller, Physics Department, University of Wisconsin, Madison, Wisconsin 53706
135. V. A. Kamath, Scientific Advisor, Attn: P. K. Patwardhan, Bhabha Atomic Research Centre, Trombay, Bombay, India
136. S. R. Kasturi, Tata Institute Fundamental Research, Bombay, 400005, India
137. R. Leach, Physics Department, University of Wisconsin, Madison, Wisconsin 53706
- 138-167. P. R. Moran, Physics Department, University of Wisconsin, Madison, Wisconsin 53706
168. D. W. Pearson, Physics Department, University of Wisconsin, Madison, Wisconsin 53706
169. E. B. Podgorsak, Physics Department, University of Wisconsin, Madison, Wisconsin 53706
170. J. N. Rogers, Division 8321, Sandia Laboratories, P.O. Box 969, Livermore, California 94550
171. M. E. Rose, Mathematics and Computer Branch, Division of Research, U.S. Atomic Energy Commission, Washington, D.C. 20545
172. J. A. Swartout, Union Carbide Corporation, New York, N.Y. 10017
173. J. Wagner, Physics Department, University of Wisconsin, Madison, Wisconsin 53706
174. Patent Office, AEC, ORO
175. Research and Technical Support Division, AEC, ORO
- 176-403. Given distribution as shown in TID-4500 under Physics category (25 copies - NTIS)